



1

Supplementary Information for

Cropland abandonment is largely fleeting, limiting its potential environmental benefits

Christopher L. Crawford, He Yin, Volker C. Radeloff, and David S. Wilcove

Corresponding Author: Christopher L. Crawford.

E-mail: ccrawford@princeton.edu

This PDF file includes:

Figs. S1 to S37 (not allowed for Brief Reports)
Tables S1 to S2 (not allowed for Brief Reports)

1 **Contents**

2	S1 Extended Results	5
3	A Limited abandonment in Mato Grosso	5
4	B Biomes	5
5	C The effect of varying abandonment definitions	5
6	D Comparing annual and two-year estimates of abandonment	5
7	E Maps of abandonment duration as of 2017 and maximum duration during time series	6
8	S2 Extended Methods	6
9	A Classifying abandonment	6
10	B Temporal filters	6
11	C Modeling abandonment decay	6
12	C.1 Model selection and diagnostics	7
13	C.2 Recultivation (“decay”) model results	7
14	D Change in recultivation rates over time	7
15	E Projecting abandonment duration into the future	7
16	S3 Supporting Tables & Figures	8
17	References	47
18	List of Tables	
19	S1 Summary statistics describing the duration of abandonment (in years) at our eleven sites between 1987 and 2017, using a five year abandonment definition, and incorporating all periods of abandonment (allowing for multiple per pixel).	8
20	S2 Cropland abandonment (in Mha) as of 2017 as identified using a) our annual time series and a five-year abandonment definition and b) a two year method taking the difference between land cover in 1987 and 2017.	9
21	List of Figures	
22	S1 The locations of our 11 sites, from Yin et al. (6). Sites are labeled as follows: (b) Vitebsk, Belarus / Smolensk, Russia; (bh) Bosnia & Herzegovina; (c) Chongqing, China; (g) Goiás, Brazil; (i) Iraq; (mg) Mato Grosso, Brazil; (n) Nebraska/Wyoming, USA; (o) Orenburg, Russia / Uralsk, Kazakhstan; (s) Shaanxi/Shanxi, China; (v) Volgograd, Russia; (w) Wisconsin, USA.	10
23	S2 Area abandoned a) as of 2017, b) at any point between 1987-2017, c) as of 2017 as a proportion of the total cropland extent (i.e., the area of all lands that were cultivated at some point during the time series). Note that sites are shown in ascending order of area abandoned as of 2017 as a proportion of total cropland extent.	11
24	S3 Cumulative area abandoned at each site through time, according to age class (in years).	12
25	S4 Area in each land cover class at each site through time. Land cover classes are cropland, grassland, woody vegetation, non-vegetation, and abandoned (for at least 5 years).	13
26	S5 Annual turnover of abandoned croplands at each site, showing the annual gain (dark green) and annual loss (i.e., recultivation, light green) and net change (black line) of abandoned croplands.	14
27	S6 The distribution of the maximum abandonment duration (in years) for each pixel at each site from 1987 to 2017. The y-scale shows the proportion of pixels with maximum duration values of a given duration at each site. As previously noted, abandonment and recultivation can occur multiple times at a single pixel during our time series, and this figure serves as a companion to the distribution of all abandonment values shown in Figure 2. Site-level mean duration values are shown in the red and blue dots, corresponding to mean values calculated across all periods of abandonment (in red, including multiple periods per pixel) and mean values calculated across only the maximum duration of abandonment at each pixel (in blue). The vertical dashed lines represent the mean of these site-level mean duration values, for all abandonment periods (red) and only the maximum duration at each pixel (blue), respectively.	15
28	S7 Maximum duration of cropland abandonment (in years) observed at each pixel between 1987 and 2017 in our eleven study sites. This serves as a companion to maps of the abandonment duration as of 2017 shown in Figure 1. Site locations are shown in Figure S1.	16
29	S8 Proportion of abandoned cropland in each land cover class as of 2017.	17

50	S9	Site biomes, using biome classifications from The Nature Conservancy's Terrestrial Ecoregions of The World (TEOW) database, derived from Olson et al. (12) and Olson and Dinerstein (13).	18
51	S10	Mean abandonment lengths shown for various abandonment thresholds.	19
52	S11	Recultivation rates shown for various abandonment thresholds.	20
53	S12	Decay model results for all sites, showing the proportion of each cohort of abandoned land (i.e., all pixels abandoned in a given year) remaining abandoned over time for each of our eleven sites. Points represent actual observations by cohort, dashed lines represent linear model predictions (fitted values) for each cohort as a function of time (including a linear and logarithmic term of time), and the solid black line represents the site-level mean trend across all cohorts (calculated by taking the mean of each time coefficient values across all cohorts, respectively, and using those two mean values to plot a mean trend). Colors of both points and dashed lines correspond to roughly five-year group of cohorts, ranging from dark purple (oldest cohorts) to green and yellow (most recent cohorts). The horizontal black dashed line shows a proportion of 0.5, indicating the point where half of a cohort has been recultivated. Model diagnostic plots are shown in Figures S14 and S15.	21
54	S13	Akaike Information Criterion (AIC) values for various recultivation ("decay") model specifications for each site. More negative AIC values indicate a better model fit.	22
55	S14	Residuals vs. fitted diagnostic plots for our linear models of the recultivation ("decay") of abandonment at each site. These models take the form shown in Equation Eq. (S2), and are shown in Figure S12.	23
56	S15	QQ plots calculated using the <code>{car}</code> package (14) for our linear models of the recultivation ("decay") of abandonment at each site. These models take the form shown in Equation Eq. (S2), and are shown in Figure S12.	24
57	S16	Mean decay model coefficients across cohorts at each site. The left panel shows the mean coefficient on the log(time) terms and the right shows the site mean coefficient on the linear time terms. These mean coefficients are used to plot the mean decay trajectories shown in Figure 3.	25
58	S17	An alternative representation of the mean decay rate for each site (also shown in Figure 3). The color of each point corresponds to the proportion remaining after a given amount of time.	26
59	S18	The rate of change of decay rates (measured as the half-life, or the time required for 50% of each cohort to be recultivated) at each site over the course of the time series. Individual site trends are shown in panel a. Solid lines show simple linear regressions, the slopes of which are shown in panel b. Gray bands around the linear trends in panel a and the error bars on slope estimates in panel b both represent 95% confidence intervals. These models are described by Eq. Eq. (S3). Model diagnostic plots are shown in Figures S19 and S20.	27
60	S19	Residuals vs. fitted diagnostic plots for each site, for a simple <code>1m</code> call corresponding to Eq. Eq. (S3), in which the half-life (i.e., the time required for half (50%) of a given cohort of abandoned cropland to be recultivated) is modeled as a function of the year of initial abandonment at each site.	28
61	S20	QQ plots calculated using the <code>car</code> package ((14)), for a simple <code>1m</code> call corresponding to Eq. Eq. (S3), in which the half-life (i.e., the time required for half (50%) of a given cohort of abandoned cropland to be recultivated) is modeled as a function of the year of initial abandonment at each site.	29
62	S21	Annual gain in newly abandoned cropland at our eleven sites. Panel a shows the trend in annual abandonment over time at each site (in 10^3 ha), and Panel b shows the mean annual abandonment (in 10^3 ha) at each site. The mean values in panel b feed into the extrapolations. Note that the annual gain in abandonment corresponds to the dark green bars in Figure S5.	30
63	S22	The results of our simple extrapolation, including a) the mean age of abandonment, and b) the total area abandoned into the future. Colors corresponding to each site are consistent across the three panels. These extrapolation assume recultivation based on the mean decay trend for each site Figure 3 and annual new abandonment based on the mean annual gain in abandonment shown in Figure S5 (dark green bars).	31
64	S23	Extrapolating area by age bin, assuming a 1) each site follows the mean recultivation ("decay") rate, and 2) a constant area abandoned each year (based on the mean annual area abandoned at each site).	32
65	S24	The results of our second extrapolation, including a) the mean age of abandonment, and b) the total area abandoned into the future. Colors corresponding to each site are consistent across the three panels. These extrapolation assume recultivation based on the mean decay trend for each site Figure 3 and annual new abandonment based on the mean annual gain in abandonment shown in Figure S5 (dark green bars).	33
66	S25	Extrapolating area by age bin, assuming a 1) each site follows the mean recultivation ("decay") rate, and 2) a constant area abandoned each year until 2017 (based on the mean annual area abandoned at each site), followed by a linearly declining area abandoned each year until reaching 0 in 2050.	34
67	S26	Comparing the mean duration of abandonment at our 11 sites observed between 1987 and 2017 with the extrapolated mean duration as of 2050 for our two extrapolations.	35
68	S27	Abandonment patterns for Vitebsk, Belarus / Smolensk, Russia, showing a) accumulation of abandoned land by age class, b) decay of abandoned land by year abandoned, c) the area in each land cover class through time (including both land that has been abandoned for five or more years, as well as any land abandoned for 1 or more years, therefore including short-term fallows), d) the annual turnover of abandoned land through time, and e) the distribution of abandonment duration for all periods of cropland abandonment (top) and the maximum duration of abandonment at each pixel (bottom).	36
69	S28	Abandonment patterns for Bosnia & Herzegovina, following Figure S27.	37

111	S29	Abandonment patterns for Chongqing, China, following Figure S27.	38
112	S30	Abandonment patterns for Goiás, Brazil, following Figure S27.	39
113	S31	Abandonment patterns for Iraq, following Figure S27.	40
114	S32	Abandonment patterns for Mato Grosso, Brazil, following Figure S27.	41
115	S33	Abandonment patterns for Nebraska/Wyoming, USA, following Figure S27.	42
116	S34	Abandonment patterns for Orenburg, Russia / Uralsk, Kazakhstan, following Figure S27.	43
117	S35	Abandonment patterns for Shaanxi/Shanxi, China, following Figure S27.	44
118	S36	Abandonment patterns for Volgograd, Russia, following Figure S27.	45
119	S37	Abandonment patterns for Wisconsin, USA, following Figure S27.	46

120 S1. Extended Results

121 Cropland abandonment at individual sites (excluding Mato Grosso, see Section S1.A.) ranged between 314,374.8 ha (Shaanxi)
122 and 930,424 ha (Orenburg) as of 2017 (Figure S3), and because our sites varied in size, this corresponded to between 7.91%
123 (Nebraska) and 19.91% (Shaanxi) of the total area of each site (Figure S2).

124 On average, we found that cropland abandonment lasted for only 14.42 years ($SD = 1.52$ years) across our time series at our
125 eleven sites. Note, however, that these summary statistics are calculated based on the mean abandonment duration at each
126 site, to account for different site sizes. The summary statistics reported are therefore the mean of the mean abandonment
127 duration at each of our eleven sites, and the standard deviation of the mean abandonment duration at each of our eleven sites.

128 We also calculated the mean standard deviation of abandonment duration across our sites, which was 7.78 years. The former
129 is a measure of the spread of mean abandonment lengths across the 11 sites, whereas the latter is a measure of the average
130 spread of abandonment lengths at each site. See Table S1.

131 The area abandoned at each site is shown in Figure S2 (see also Table S2). The area abandoned at each site, by age class,
132 is shown in Figure S3, and the area in each land cover class at each site is shown in Figure S4. Figure S3 shows that the
133 timing of abandonment varied across sites; some sites showed more abandonment earlier in the time series (e.g., Iraq; Bosnia &
134 Herzegovina; Volgograd, Russia; Nebraska/Wyoming, USA; & Mato Grosso, Brazil), some showed consistent abandonment over
135 time (e.g., Vitebsk, Belarus/Smolensk, Russia; Goiás, Brazil; and Wisconsin, USA), and others showed increasing abandonment
136 later on in the time series (e.g., sites in Shaanxi/Shanxi and Chongqing, China). Furthermore, Figure S5 shows the annual
137 gain, loss, and net change in the area of abandoned croplands abandoned at each site.

138 **A. Limited abandonment in Mato Grosso.** Mato Grosso, Brazil, was the only site that did not experience significant amounts of
139 cropland abandonment during our time series. This is unsurprising given the recent history of agriculturally-driven land-use
140 change over the last few decades. That being said, the abandonment that did take place in Mato Grosso was relatively more
141 durable, requiring 25 years to decline by half and 110 years for complete turnover. However, because Mato Grosso showed large
142 amounts of new cultivation over the course of our time series and relatively little abandonment (9,006 ha, or 0.47% of the total
143 cropland extent, as of 2017), these results should be interpreted with care.

144 **B. Biomes.** Some ecosystems and biomes seem to recover more quickly than others, namely in relatively higher latitudes,
145 relatively colder climates, and in relatively more humid biomes (1). Our sites cover a range of biomes (Figure S9), including:

- 146 • Temperate Broadleaf and Mixed Forests (Vitebsk Belarus/Smolensk, Russia; Bosnia & Herzegovina; Wisconsin, USA),
- 147 • Temperate Grasslands, Savannas, and Shrublands (Nebraska/Wyoming, USA; Orenburg, Russia/Uralsk, Kazakhstan;
148 Volgograd, Russia),
- 149 • Tropical Grassland (Goiás and Mato Grosso, Brazil),
- 150 • Tropical Moist Broadleaf Forests (Chongqing, China; Mato Grosso, Brazil),
- 151 • Montane Grassland and Shrublands (Shaanxi/Shanxi, China), and
- 152 • Deserts & Xeric Shrublands (Iraq).

153 The long-term land-cover outcomes for abandoned croplands are shown (as of 2017) in Figure S8. Land cover outcomes for
154 abandoned croplands showed wide variation across sites, with most abandonment in Wisconsin being classified as forest by
155 2017 (60% forest, 40% grassland), but remaining mostly in grassland elsewhere (Figure S8). This limited woody vegetation
156 regrowth may be a product of the biome, but it may simply be a result of insufficient time for woody biomass to develop. Land
157 cover alone cannot confidently serve as a proxy for ecosystem recovery.

158 **C. The effect of varying abandonment definitions.** A relatively short-term definition of abandonment might result in an
159 overestimation of recultivation, because short-term abandonment may be better understood as cyclical fallow periods, not
160 true abandonment (2). Because typical fallow period length may vary around the world, we tested multiple abandonment
161 thresholds in order to test the sensitivity of our results to our choice of a five-year abandonment definition, following the FAO
162 (3). As our abandonment threshold increased in length, the mean abandonment duration across our sites increased accordingly,
163 ranging between 7 years (no threshold) and 19 years (10-year threshold). As expected, using a longer abandonment definition
164 reduced the amount of cropland abandonment we detected, which is also shown in the area in the different colored age classes
165 in Figure S3.

166 The proportion of abandoned croplands that were recultivated by the end of the time series also responded to our abandonment
167 threshold, with less recultivation for longer abandonment thresholds (Figure S11). However, even at the longest abandonment
168 definition (10 years), we still saw that between 10% and 30% of abandoned croplands were recultivated by the end of the time
169 series. We find that the mean area of abandoned croplands that get recultivated by the end of the time series declines from
170 37.77% with a 5 year threshold to 30.93% with a 7 year threshold, and 22.83% with a 10 year threshold. This indicates that
171 the abandonment and recultivation we observe is not merely a function of our five-year abandonment definition.

172 **D. Comparing annual and two-year estimates of abandonment.** Some studies estimate cropland abandonment by simply looking
173 for areas where land cover is classified as “cultivated” in one year, but not in a later year (e.g., 1992 and 2015 in ref. (4)).
174 In order to understand the magnitude of the differences that could result from using this two-year approach, we estimated
175 cropland abandonment by simply identifying areas that were classified as “cropland” in 1987 and classified as either “woody
176 vegetation” or “herbaceous vegetation” in 2017 (i.e., excluding “non-vegetation”).

177 Table S2 shows the area of abandoned croplands as identified using a five-year abandonment definition and the full annual
178 time series (Column 2), and the area of abandoned croplands identified using only the difference between 2017 and 1987
179 (Column 3). These two methods produced abandonment area estimates that ranged between 39.75% lower (Goiás, Brazil) and
180 83.29% higher (Mato Grosso, Brazil) than the abandoned area identified using the full time series.

181 Not only do these methods produce different area estimates, but they also differ in the location of the abandonment they
182 identify, with spatial agreement of only 28.08% (Mato Grosso, Brazil) to 66.3% (Bosnia & Herzegovina) (see Table S2). We
183 measure spatial agreement using the Jaccard similarity index [Legendre2012], a measure of overlap between two sets, defined as
184 the proportion of shared elements, or the intersection divided by the union (Equation Eq. (S1)) (5):

$$J(a, b) = \frac{a \cap b}{a \cup b} \quad [S1]$$

186 **E. Maps of abandonment duration as of 2017 and maximum duration during time series.** As described in the main text, because
187 a pixel may be abandoned and recultivated multiple times throughout the time series, we calculated the mean abandonment
188 duration in two ways: 1) across all periods of abandonment (as shown in Figure 2), and 2) across only the longest period of
189 abandonment experienced by each pixel. Maps of the maximum abandonment duration at each pixel at each site is shown in
190 Figure S7 (serving as a companion to Figure 1). The distribution of maximum duration values, and the corresponding mean
191 maximum duration value at each site, is shown in Figure S6 (serving as a companion to Figure 2).

192 Expanded site-specific results are shown in Figures S27-S37.

193 **S2. Extended Methods**

194 As noted in our main text, we build on annual land cover maps for 1987-2017 developed by Yin et al. (6). The following section
195 outlines our data processing and analytical methods in more specific detail than was possible in the main text. We processed
196 and analyzed our abandonment map data in RStudio version 1.4.1717 (7), using R version 4.1.0 (2021-05-18), relying heavily
197 on the `{raster}` (8), `{terra}` (9), `{data.table}` (10), and `{tidyverse}` (11) packages.

198 **A. Classifying abandonment.** Pixels that remained in cropland or non-cropland classes throughout the entire time series were
199 excluded, as were periods of non-cropland that began in the first year of the time series, even if that pixel was later classified
200 as cropland and subsequently abandoned. In effect, we only counted periods of abandonment that we could verify had followed
201 agricultural activity during our time series.

202 As noted, pixels that transitioned from cropland to the non-vegetation land cover class were not considered “abandoned,”
203 and therefore we excluded all non-vegetation pixels from our entire analysis. These pixels accounted for <10% of total site area
204 at all sites except Shaanxi (12.7%) and Iraq (52.8%), and remained stable or declined over time at all eleven sites (see Figure
205 S4).

206 All area calculations were performed using the `{terra}` package’s `cellSize()` function, which calculates the spherical area
207 of each cell as defined by its four corners (9).

208 **B. Temporal filters.** In order to address potential classification errors in a single year, we implemented a series of temporal
209 filters designed to smooth trajectories by looking for short-term land-cover changes that are temporally unlikely. We applied
210 five-year and eight-year moving-window filters that searched for short periods of land cover classifications that do not match
211 those immediately before and after, and subsequently updated them to match the surrounding classifications. Specifically, the
212 five-year filter searched for one year periods that did not match the two years immediately before and after (i.e., patterns of
213 11011, where 1 represents non-cropland and 0 represents cropland), and our eight-year filter searched for two year periods that
214 did not match the three years before and after (i.e., 11100111). The central classifications were then updated to match the
215 classes on either end.

216 **C. Modeling abandonment decay.** Our mean abandonment duration metric tells us about the general persistence of abandoned
217 croplands throughout the time series. However, this value is limited by the time series length, and does not account for when
218 the majority of the abandonment took place at a site, nor whether a period of abandonment ends as a result of recultivation
219 or the end of the time series. As a result, the mean abandonment duration does not tell us how long to expect a piece of land
220 to remain abandoned, nor how abandonment length varies through time. To address this constraint, we track the trajectory of
221 each pixel through time following its initial abandonment, grouping pixels abandoned in a given year into “cohorts.” Decay
222 rates provide information about how long it takes for land to be recultivated, complementing the mean abandonment length
223 and providing a more nuanced story about how long to expect abandonment to last.

224 For example, a site may have a relatively short mean length of abandonment (e.g., Shaanxi/Shanxi [China], with a mean
225 abandonment length of 13 years; see Figure 1), but also have a gradual decay rate, indicating that land should stay abandoned
226 for a relatively longer amount of time. This may result from more abandonment occurring towards the end of the time series;
227 this land simply does not have as long to age and shows up as younger in our data, regardless of how long it may last. Looking
228 at abandonment decay rates for each cohort individually allows us to produce a decay rate for each site in general in a way
229 that accounts for when during the time series a piece of land was abandoned (i.e., giving us a sense of how long to expect a
230 given piece of land to remain abandoned, even into the future).

231 **C.1. Model selection and diagnostics.** We fit linear models using the `lm()` function in R's core statistics package `{stats}`, predicting
 232 the proportion of abandoned cropland in each cohort remaining abandoned as a function of time since initial abandonment at
 233 each site. The proportion of abandoned cropland remaining abandoned is measured relative to the area abandoned 5 years
 234 following the year of initial abandonment, as dictated by our five year abandonment definition.

235 We tested a range of model specifications, including linear and log transformations of both *proportion* and *time*. Due to a
 236 linear relationship between model residuals and time when including only one term for *time*, we also tested models containing
 237 multiple *time* predictor terms, including both log and linear terms.

238 We chose a model with the following specifications shown in Equation 1 and reproduced here in Equation Eq. (S2). For
 239 cohorts of abandonment initially abandoned in years $y = 1988, \dots, 2013$, we estimate the proportion p of each cohort y remaining
 240 abandoned as a function of time t (i.e., based on the number of years after initial abandonment).

$$p_y = 1 + \beta_{1,y} \log(t+1) + \beta_{2,y} t \quad [S2]$$

242 Where $\beta_{1,y}$ represents the regression coefficient on the log term of time t for cohort y , and $\beta_{2,y}$ represents the regression
 243 coefficient on the linear term of time t for cohort y . We allow for *cohort* level fixed effects, fitting unique coefficients for each
 244 cohort at each site. We ran individual models for each site, using a `stats::lm()` call of `lm(formula = I(proportion - 1) ~`
 245 `0 + log(time + 1):cohort + I(time):cohort)` on data for only that site. Taken together, these 11 models are correspond to
 246 a `stats::lm()` call of `lm(formula = I(proportion - 1) ~ 0 + log(time + 1):cohort:site + I(time):cohort:site)`.

247 Model selection was performed based on Akaike Information Criterion (AIC) values (Figure S13), selecting the model with
 248 the lowest (i.e., more negative) AIC value. We confirmed that linear model assumptions were not violated through visual
 249 inspection of both residuals vs. fitted plots (Figure S14) and Q-Q plots (Figure S15).

250 **C.2. Recultivation (“decay”) model results.** The observed data, fitted values from these linear models, and mean decay rates for
 251 each site, are shown in Figure S12.

252 In order to calculate the mean decay trajectory at each site (as shown in Figure 3), we took the mean of the log coefficients
 253 ($\beta_{1,\bar{y}}$) and the linear coefficients ($\beta_{1,\bar{y}}$) respectively across all cohorts y at each site. These mean values are shown in Figure
 254 S16. We then used these mean coefficient values ($\beta_{1,\bar{y}}$ and $\beta_{1,\bar{y}}$) to define a new function describing the mean recultivation (or
 255 decay) trajectory at each site, using the same for as Equation Eq. (S2).

256 An alternative representation of the mean recultivation rate is shown in Figure S17.

257 **D. Change in recultivation rates over time.** We examined the rate of change of recultivation rates by calculating the half-life,
 258 $t_{half,s}$, defined as the time required for half (50%) of a given cohort of abandoned cropland to be recultivated, and parameterizing
 259 a simple linear model on these half-life values as a function of time, using the `stats::lm()` function in R's core statistics
 260 package `{stats}`. We estimate the half-life, $t_{half,s}$, as a function of the year of initial abandonment ($yearabn_s$), at each site s ,
 261 as shown in Equation Eq. (S3).

$$t_{half,s} = \beta_{0,s} + \beta_{1,s} yearabn_s \quad [S3]$$

262 Where $\beta_{1,s}$ represents the regression slope on the year abandoned (cohort) for site s ($yearabn_s$), and $\beta_{0,s}$ represents the
 263 intercept. This corresponds to a `stats::lm()` call of `lm(formula = t_half ~ year_abandoned)`, run for each site individually.
 264 Results are shown in Figure S18.

265 We confirmed that model assumptions were met through visual inspection of residuals vs. fitted plots (Figure S19) and Q-Q
 266 plots (Figure S20).

267 **E. Projecting abandonment duration into the future.** The results of the projection highlighted in the main text (referred to here
 268 as “Extrapolation 1”) are shown in Figure S22 and Figure S23. As noted in the main text, we make two simple assumptions in
 269 our projection of abandonment and recultivation into the future: specifically, that 1) recultivation rates remain the same (based
 270 on mean recultivation trends at each site, shown in Figure 3, and that 2) a constant amount of cropland is newly abandoned
 271 each year, based on the mean annual gain in abandonment shown in Figure S21b (note: the annual gain in abandonment in
 272 Figure S21a corresponds to the dark green bars in Figure S5).

273 Given that abandonment may not continue indefinitely, we also explore an alternative to our second assumption about the
 274 amount of additional abandonment each year. In this alternative assumption (“Extrapolation 2”), the area abandoned each
 275 year is the same as “Extrapolation 1” from 1987-2017, based on the mean annual gain in abandonment (Figure S21b), but
 276 linearly declines between 2017-2050, reaching 0 ha at each site in 2050 (see Figures S24 and S25).

277 While mean age of abandoned land increased through time after 2017 (and most dramatically after 2050), it remained below
 278 37 years at all sites by 2050. Increases in mean abandonment duration were offset by recultivation, and total area abandoned
 279 declined quickly after 2020 at most sites. The mean abandonment duration increases as annual abandonment declines, as the
 280 total pool of abandoned land grows older and is gradually recultivated.

282 **S3. Supporting Tables & Figures**

Table S1. Summary statistics describing the duration of abandonment (in years) at our eleven sites between 1987 and 2017, using a five year abandonment definition, and incorporating all periods of abandonment (allowing for multiple per pixel).

Site	Mean	Median	Standard Deviation
Vitebsk, Belarus / Smolensk, Russia	13.87	12	7.60
Bosnia & Herzegovina	17.70	18	8.36
Chongqing, China	12.92	11	7.32
Goiás, Brazil	13.61	12	7.42
Iraq	15.72	13	8.78
Mato Grosso, Brazil	15.30	11	9.21
Nebraska/Wyoming, USA	15.32	14	8.04
Orenburg, Russia / Uralsk, Kazakhstan	12.86	11	6.95
Shaanxi/Shanxi, China	13.00	11	7.15
Volgograd, Russia	13.33	12	7.01
Wisconsin, USA	15.00	14	7.78

Table S2. Cropland abandonment (in Mha) as of 2017 as identified using a) our annual time series and a five-year abandonment definition and b) a two year method taking the difference between land cover in 1987 and 2017.

Site	Area (annual, as of 2017)	Area (two year: 2017-1987)	Percent Difference	Jaccard Similarity
Goiás, Brazil	530,252	319,499	-39.75%	0.29
Vitebsk, Belarus / Smolensk, Russia	917,934	655,689	-28.57%	0.51
Chongqing, China	382,125	273,839	-28.34%	0.43
Nebraska/Wyoming, USA	351,006	274,133	-21.9%	0.50
Bosnia & Herzegovina	690,376	569,091	-17.57%	0.66
Wisconsin, USA	411,833	358,420	-12.97%	0.48
Iraq	368,103	348,152	-5.42%	0.54
Volgograd, Russia	828,276	857,989	3.59%	0.47
Orenburg, Russia / Uralsk, Kazakhstan	930,424	975,131	4.8%	0.52
Shaanxi/Shanxi, China	314,375	355,581	13.11%	0.49
Mato Grosso, Brazil	9,006	16,507	83.29%	0.28

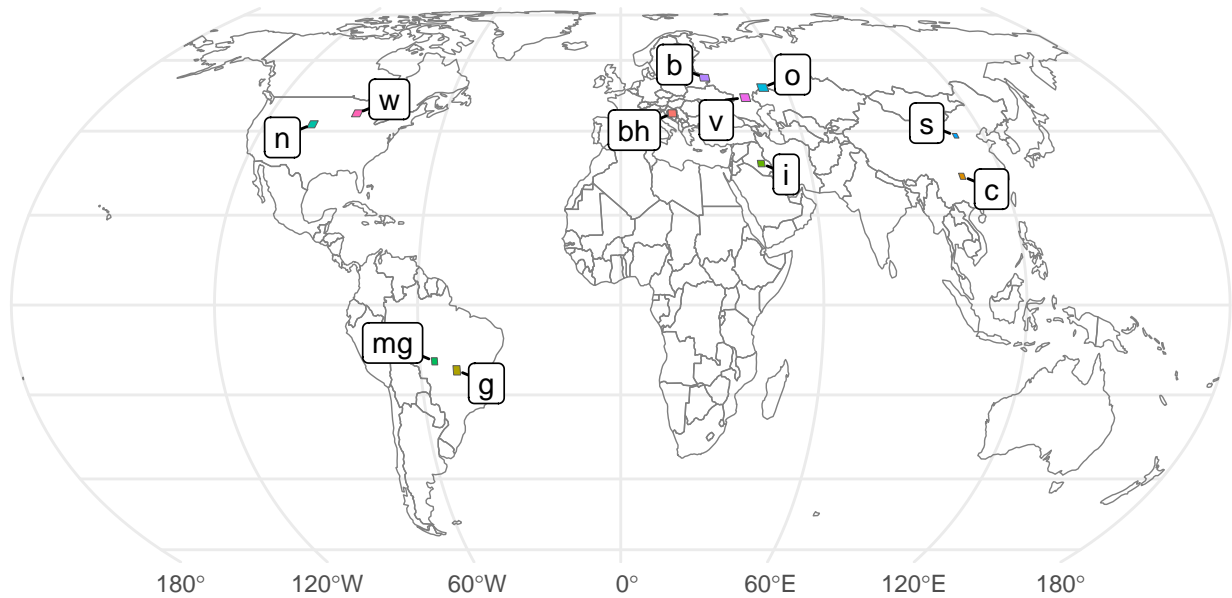


Fig. S1. The locations of our 11 sites, from Yin et al. (6). Sites are labeled as follows: (b) Vitebsk, Belarus / Smolensk, Russia; (bh) Bosnia & Herzegovina; (c) Chongqing, China; (g) Goiás, Brazil; (i) Iraq; (mg) Mato Grosso, Brazil; (n) Nebraska/Wyoming, USA; (o) Orenburg, Russia / Uralsk, Kazakhstan; (s) Shaanxi/Shanxi, China; (v) Volgograd, Russia; (w) Wisconsin, USA.

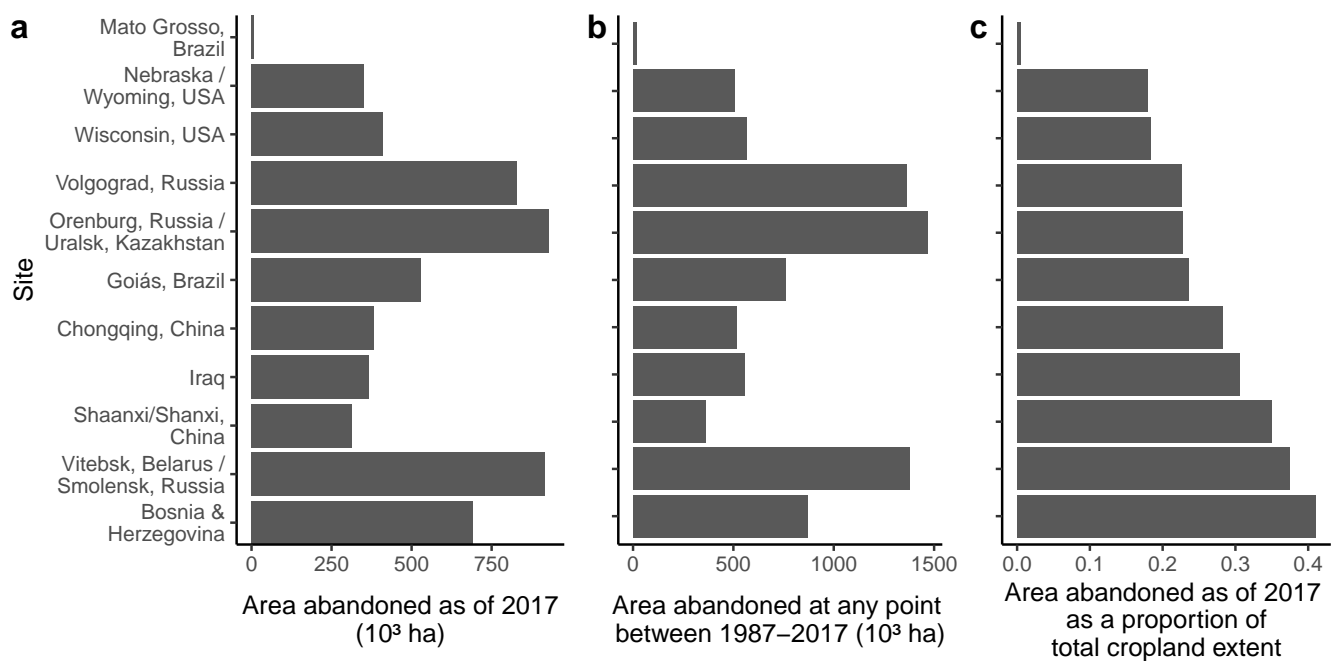


Fig. S2. Area abandoned a) as of 2017, b) at any point between 1987–2017, c) as of 2017 as a proportion of the total cropland extent (i.e., the area of all lands that were cultivated at some point during the time series). Note that sites are shown in ascending order of area abandoned as of 2017 as a proportion of total cropland extent.

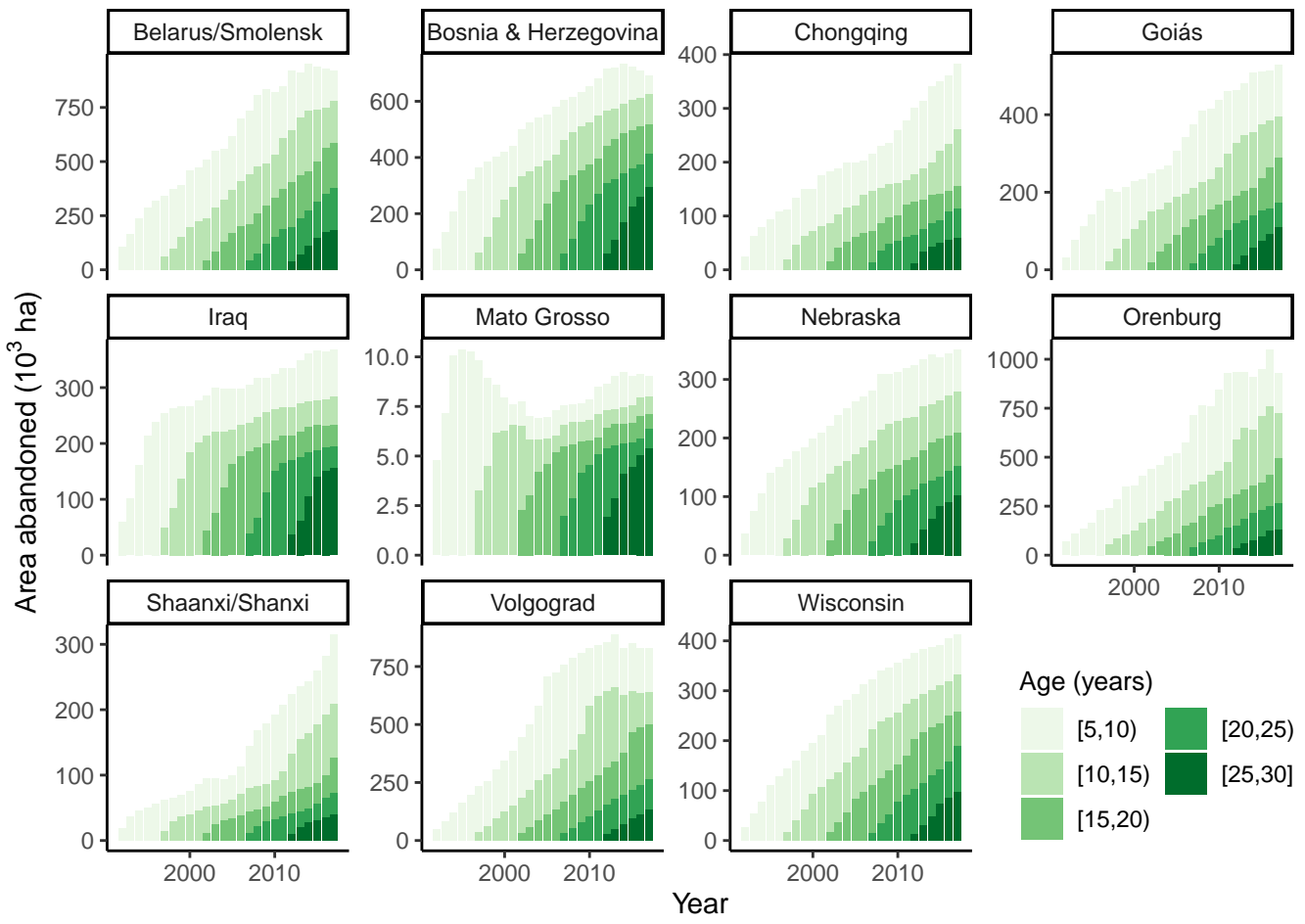


Fig. S3. Cumulative area abandoned at each site through time, according to age class (in years).

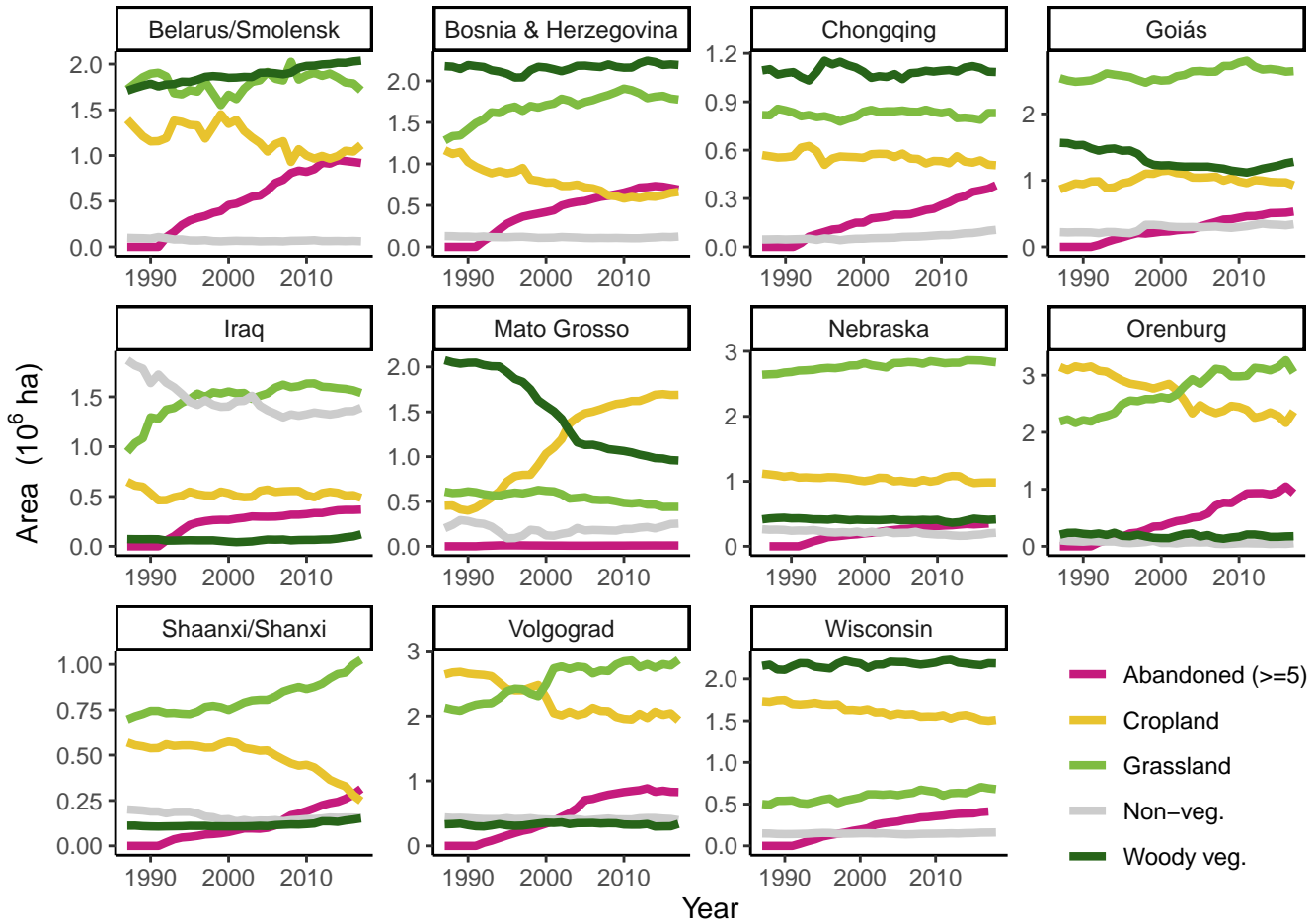


Fig. S4. Area in each land cover class at each site through time. Land cover classes are cropland, grassland, woody vegetation, non-vegetation, and abandoned (for at least 5 years).

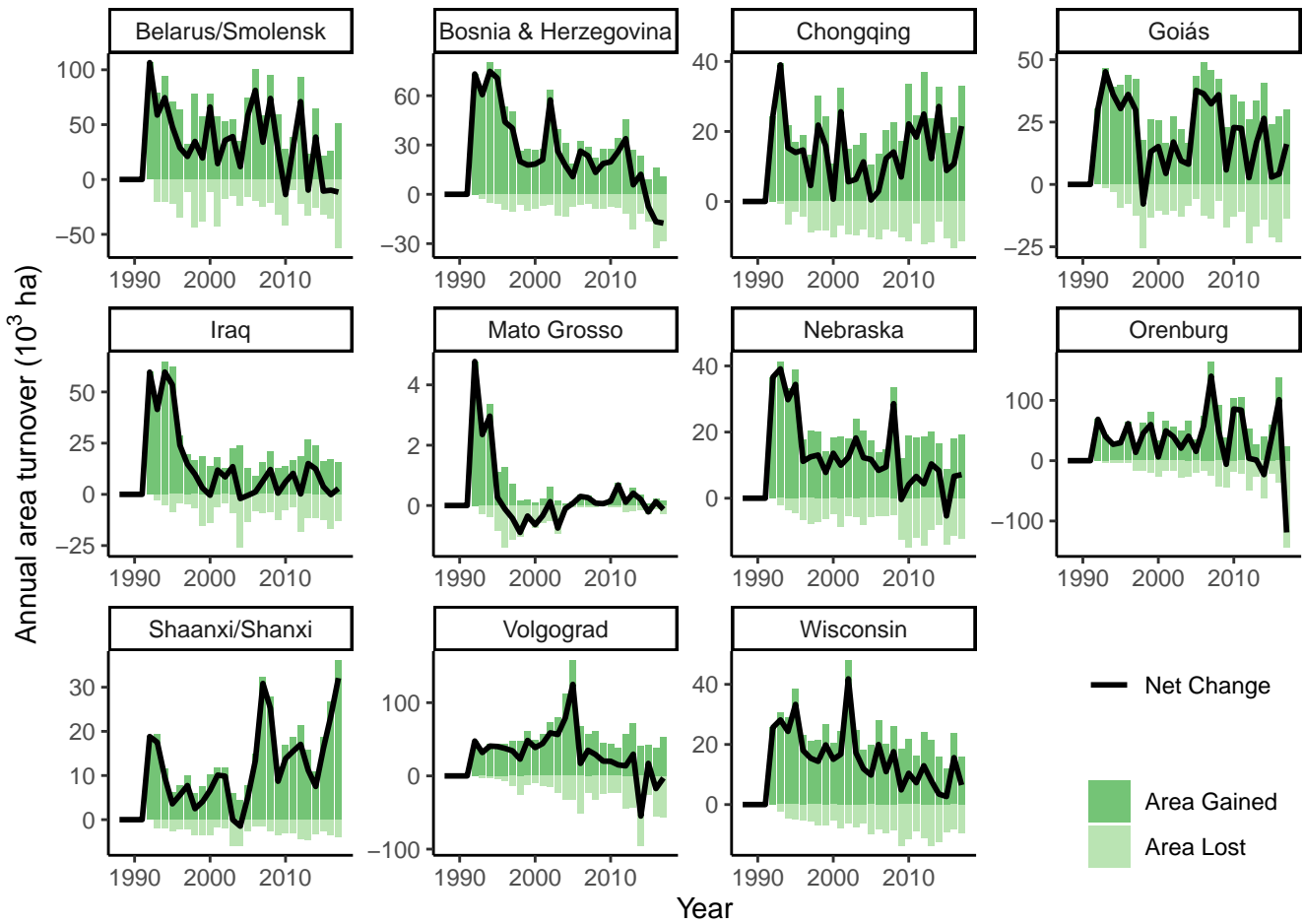


Fig. S5. Annual turnover of abandoned croplands at each site, showing the annual gain (dark green) and annual loss (i.e., recultivation, light green) and net change (black line) of abandoned croplands.

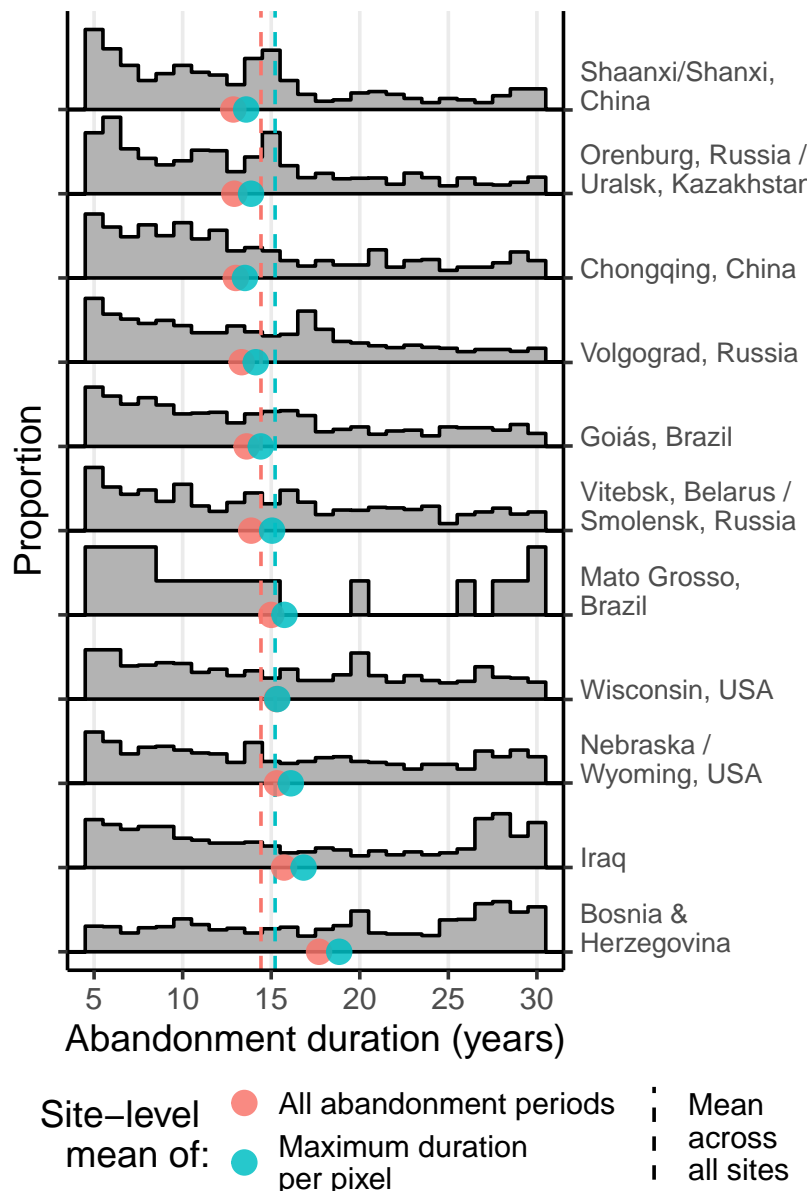


Fig. S6. The distribution of the maximum abandonment duration (in years) for each pixel at each site from 1987 to 2017. The y-scale shows the proportion of pixels with maximum duration values of a given duration at each site. As previously noted, abandonment and recultivation can occur multiple times at a single pixel during our time series, and this figure serves as a companion to the distribution of all abandonment values shown in Figure 2. Site-level mean duration values are shown in the red and blue dots, corresponding to mean values calculated across all periods of abandonment (in red, including multiple periods per pixel) and mean values calculated across only the maximum duration of abandonment at each pixel (in blue). The vertical dashed lines represent the mean of these site-level mean duration values, for all abandonment periods (red) and only the maximum duration at each pixel (blue), respectively.

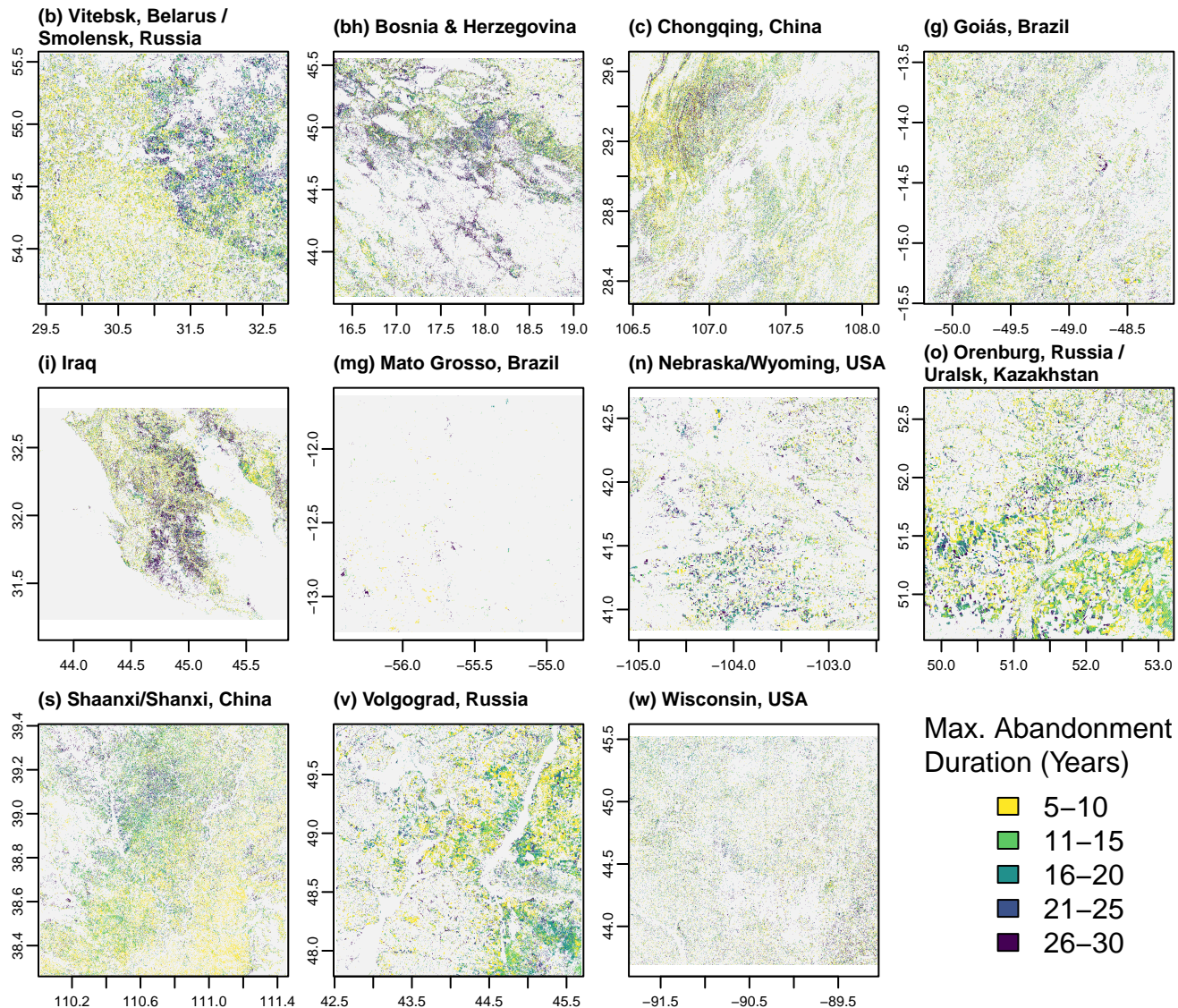


Fig. S7. Maximum duration of cropland abandonment (in years) observed at each pixel between 1987 and 2017 in our eleven study sites. This serves as a companion to maps of the abandonment duration as of 2017 shown in Figure 1. Site locations are shown in Figure S1.

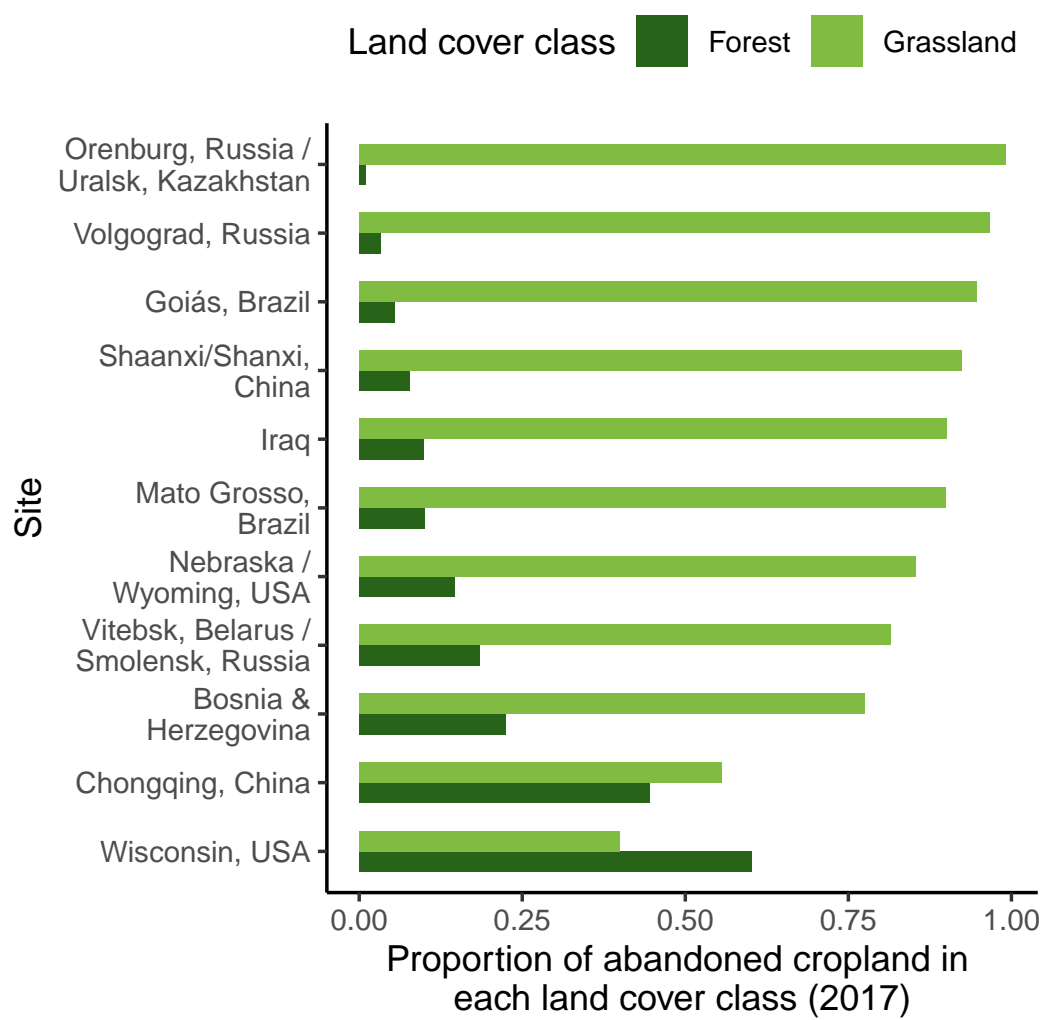


Fig. S8. Proportion of abandoned cropland in each land cover class as of 2017.

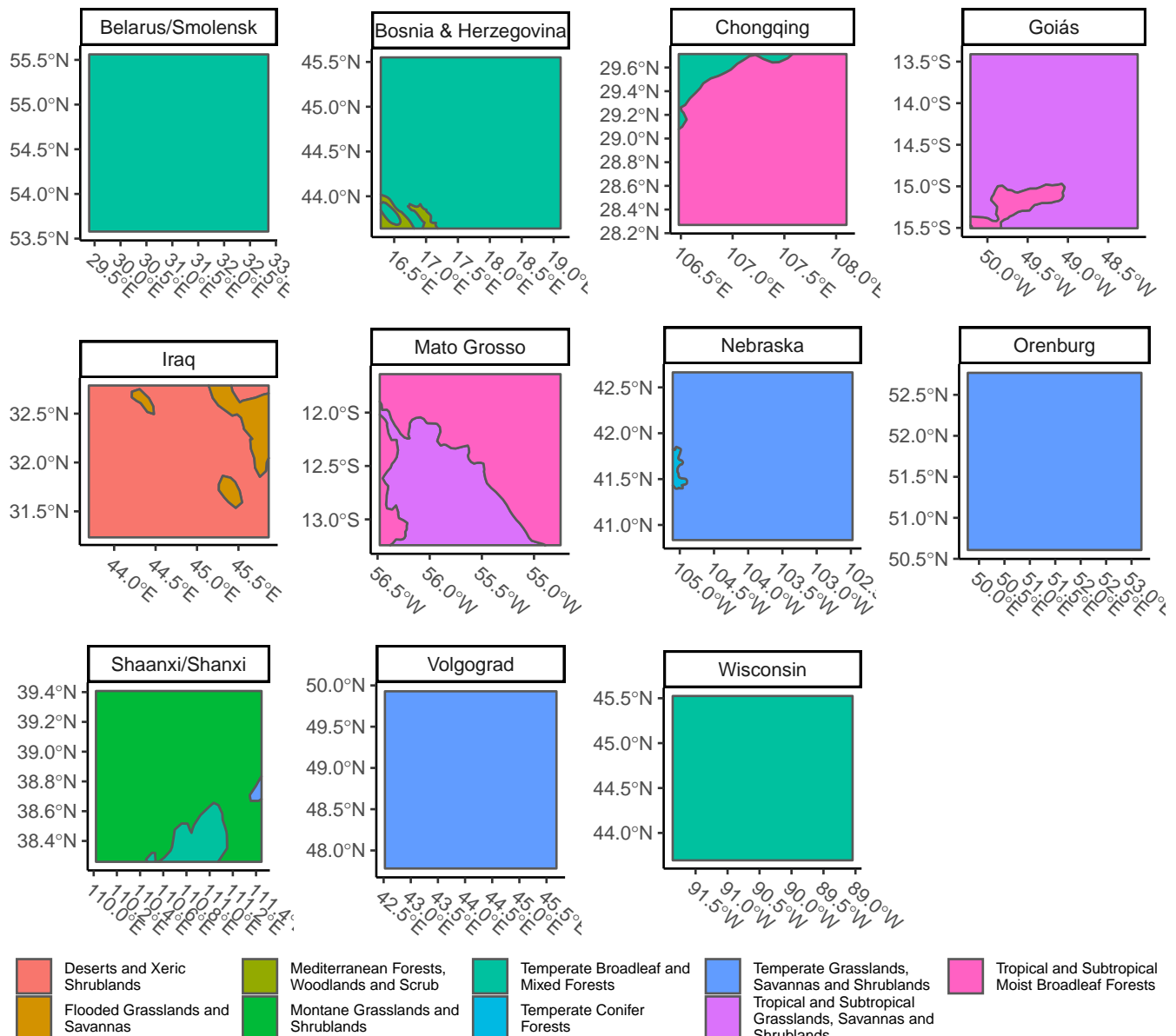


Fig. S9. Site biomes, using biome classifications from The Nature Conservancy's Terrestrial Ecoregions of The World (TEOW) database, derived from Olson et al. (12) and Olson and Dinerstein (13).

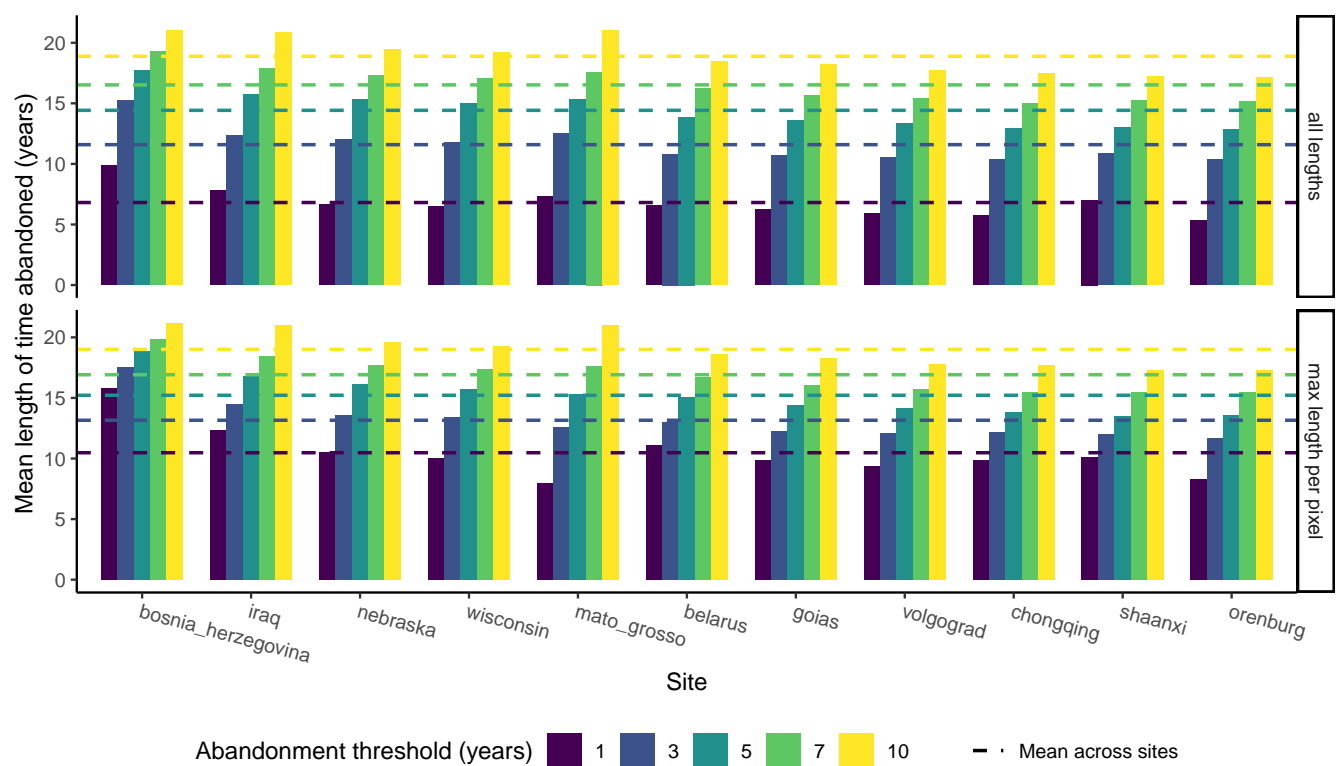


Fig. S10. Mean abandonment lengths shown for various abandonment thresholds.

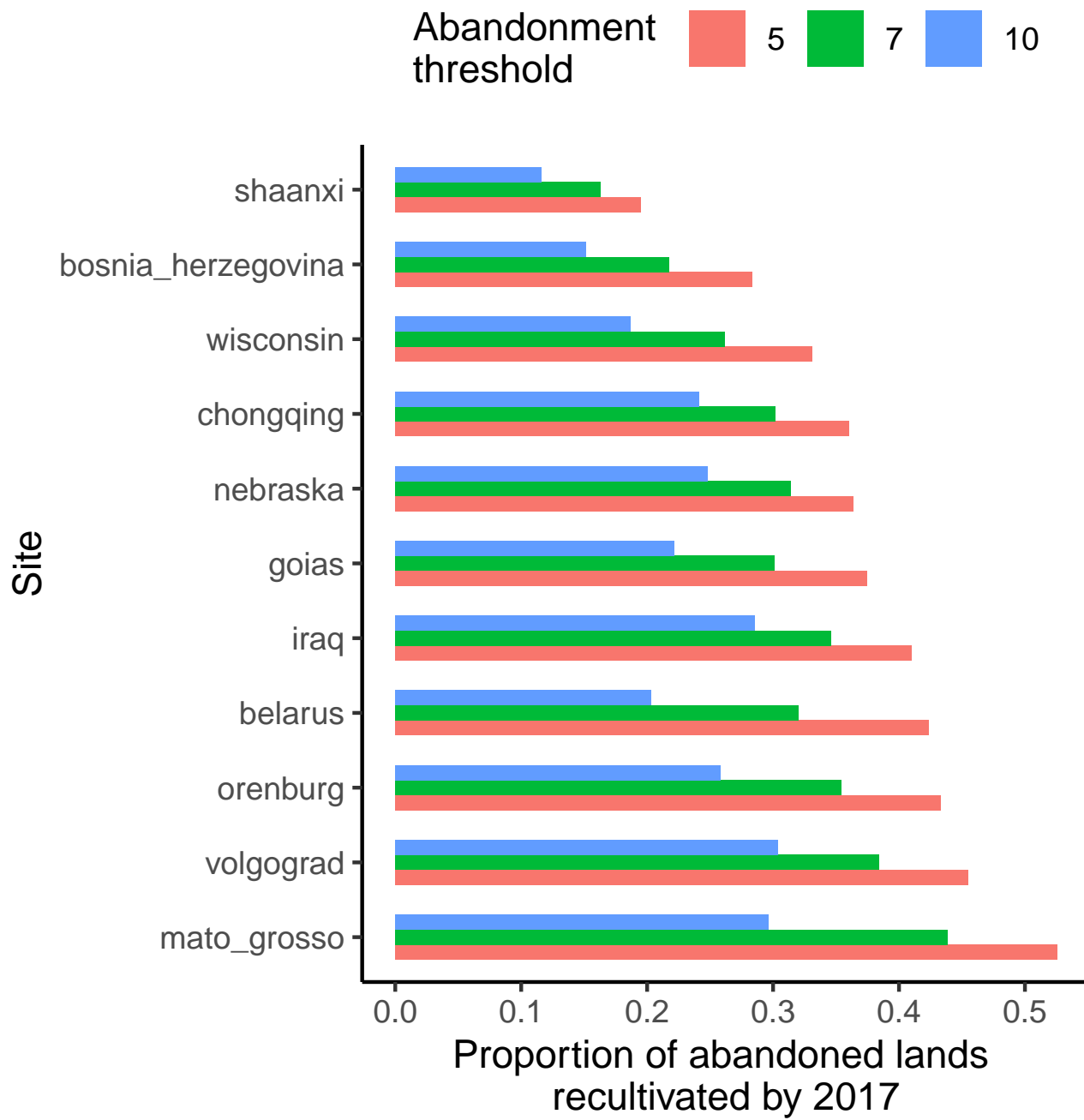


Fig. S11. Recultivation rates shown for various abandonment thresholds.

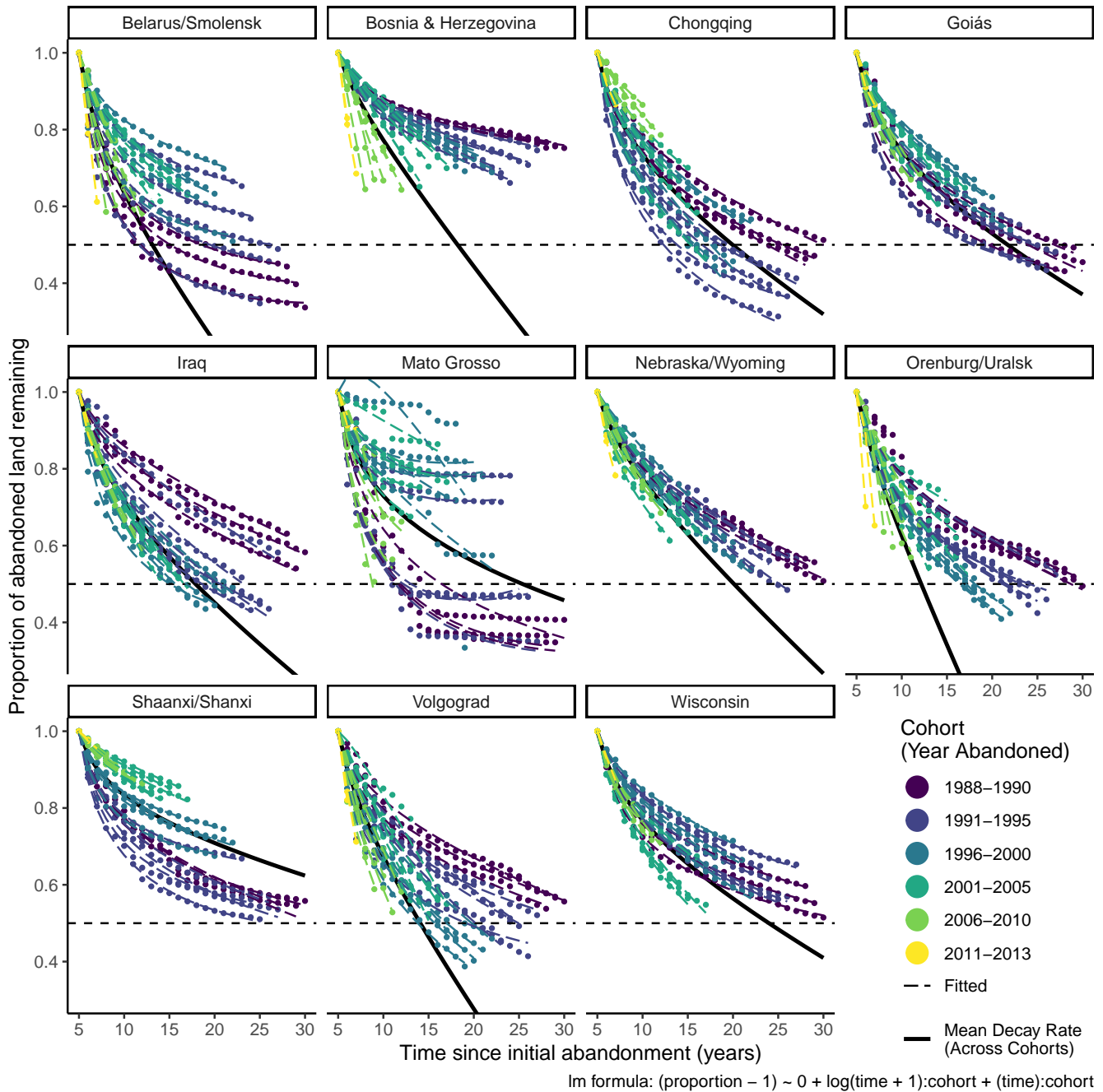


Fig. S12. Decay model results for all sites, showing the proportion of each cohort of abandoned land (i.e., all pixels abandoned in a given year) remaining abandoned over time for each of our eleven sites. Points represent actual observations by cohort, dashed lines represent linear model predictions (fitted values) for each cohort as a function of time (including a linear and logarithmic term of time), and the solid black line represents the site-level mean trend across all cohorts (calculated by taking the mean of each time coefficient values across all cohorts, respectively, and using those two mean values to plot a mean trend). Colors of both points and dashed lines correspond to roughly five-year group of cohorts, ranging from dark purple (oldest cohorts) to green and yellow (most recent cohorts). The horizontal black dashed line shows a proportion of 0.5, indicating the point where half of a cohort has been recultivated. Model diagnostic plots are shown in Figures S14 and S15.

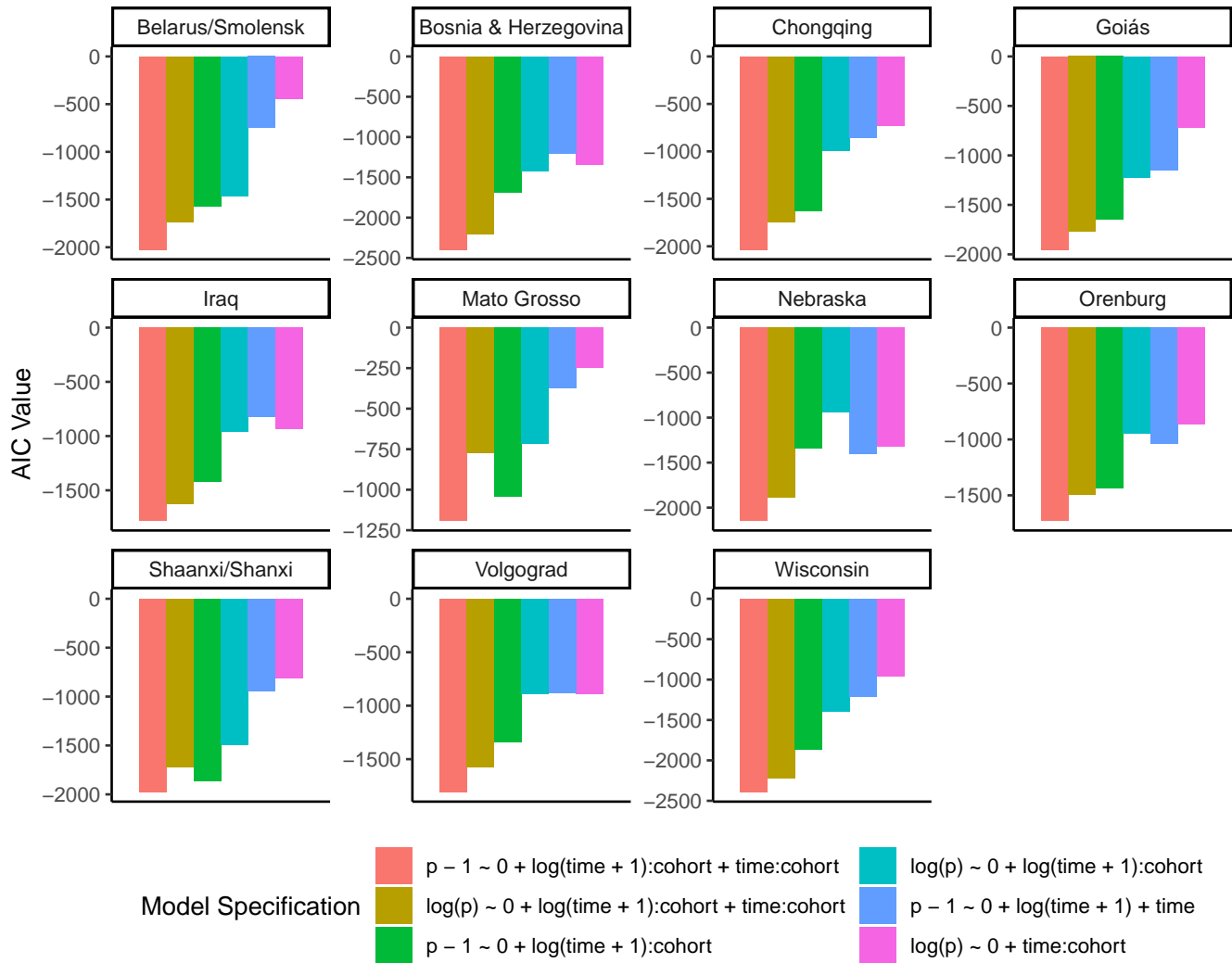


Fig. S13. Akaike Information Criterion (AIC) values for various recultivation ("decay") model specifications for each site. More negative AIC values indicate a better model fit.

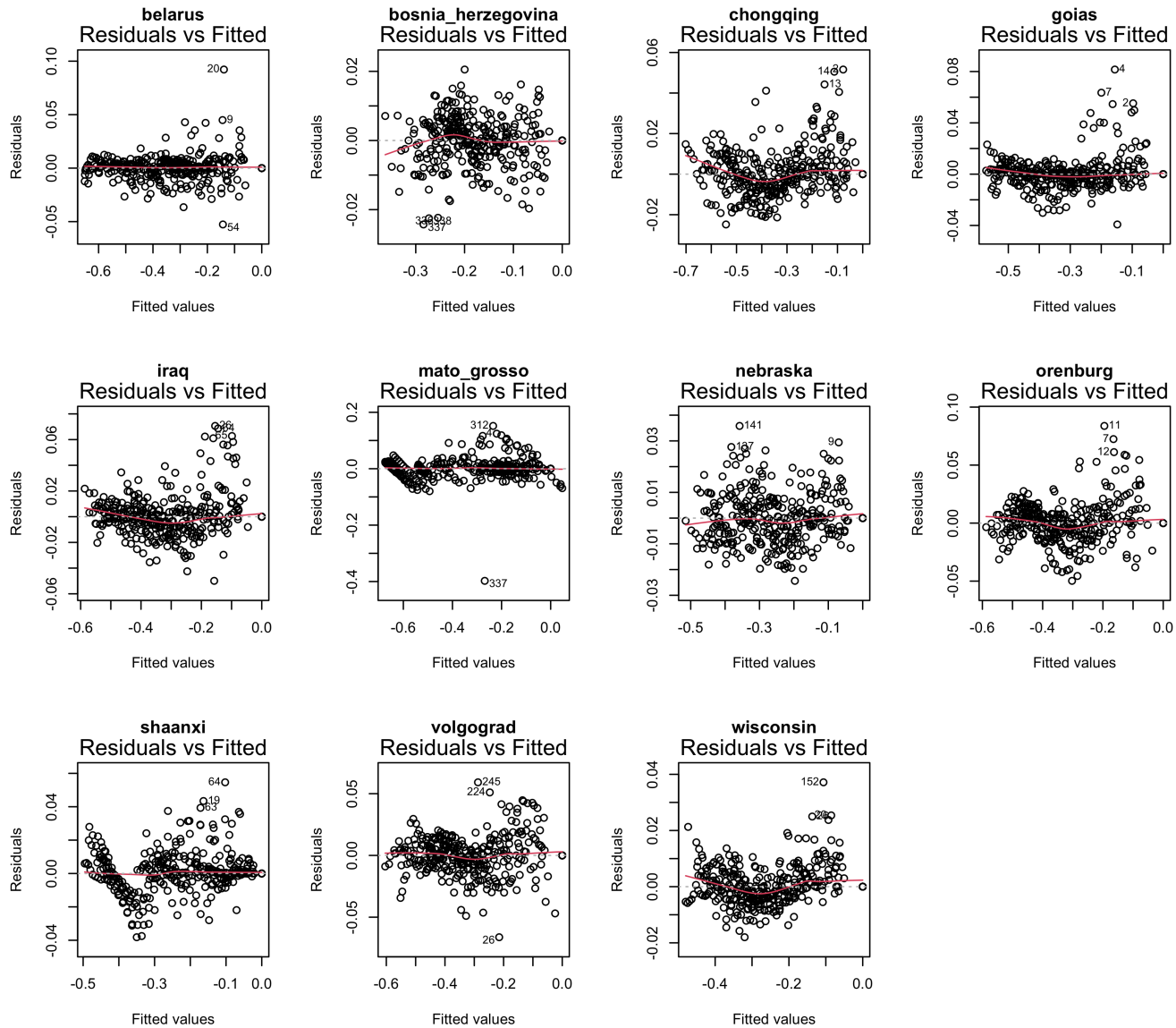


Fig. S14. Residuals vs. fitted diagnostic plots for our linear models of the recultivation ("decay") of abandonment at each site. These models take the form shown in Equation Eq. (S2), and are shown in Figure S12.

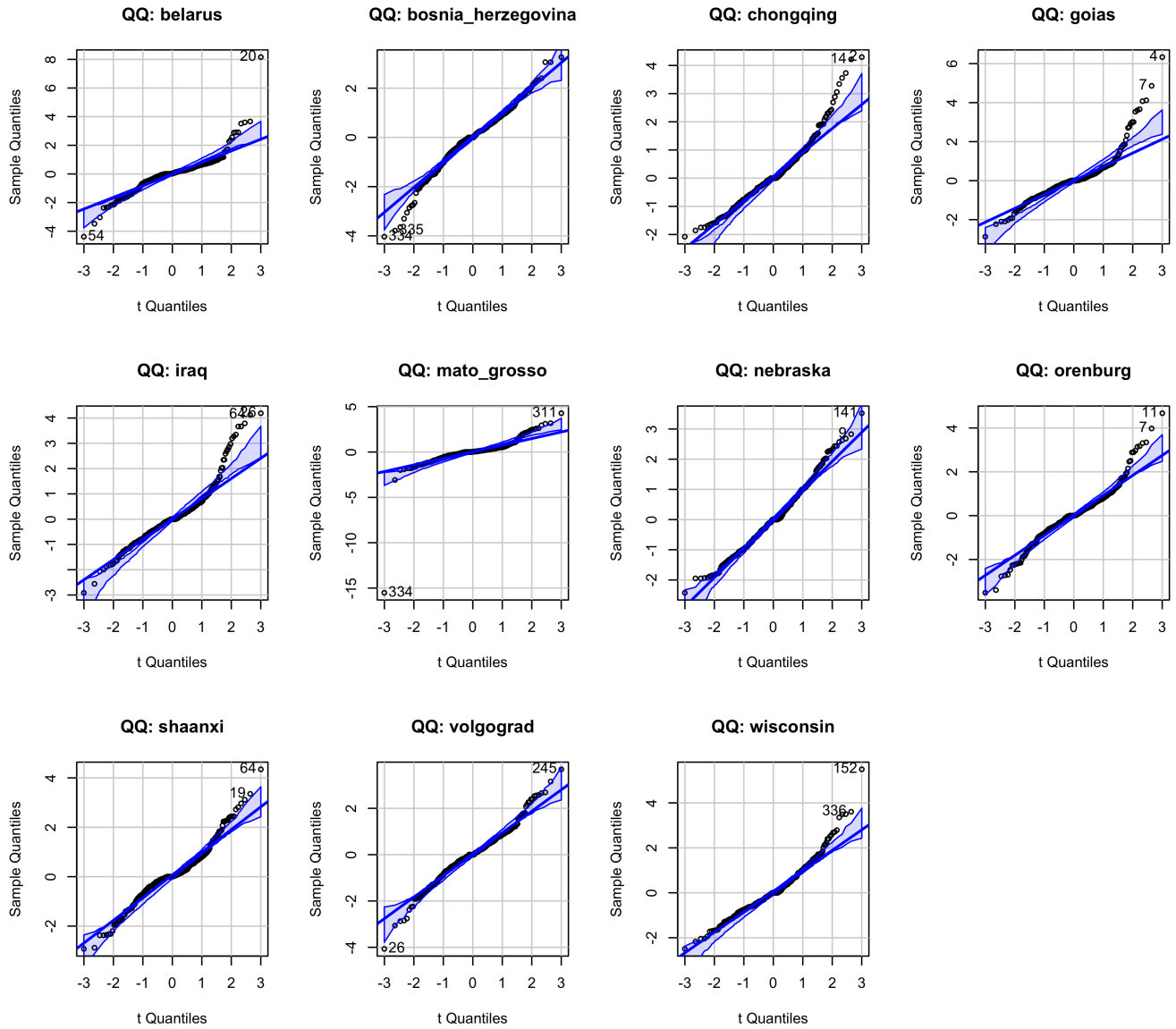


Fig. S15. QQ plots calculated using the `{car}` package (14) for our linear models of the recultivation ("decay") of abandonment at each site. These models take the form shown in Equation Eq. (S2), and are shown in Figure S12.

Mean Decay Rates By Site

Im formula: $(\text{proportion} - 1) \sim 0 + \log(\text{time} + 1):\text{cohort} + (\text{time}):\text{cohort}$

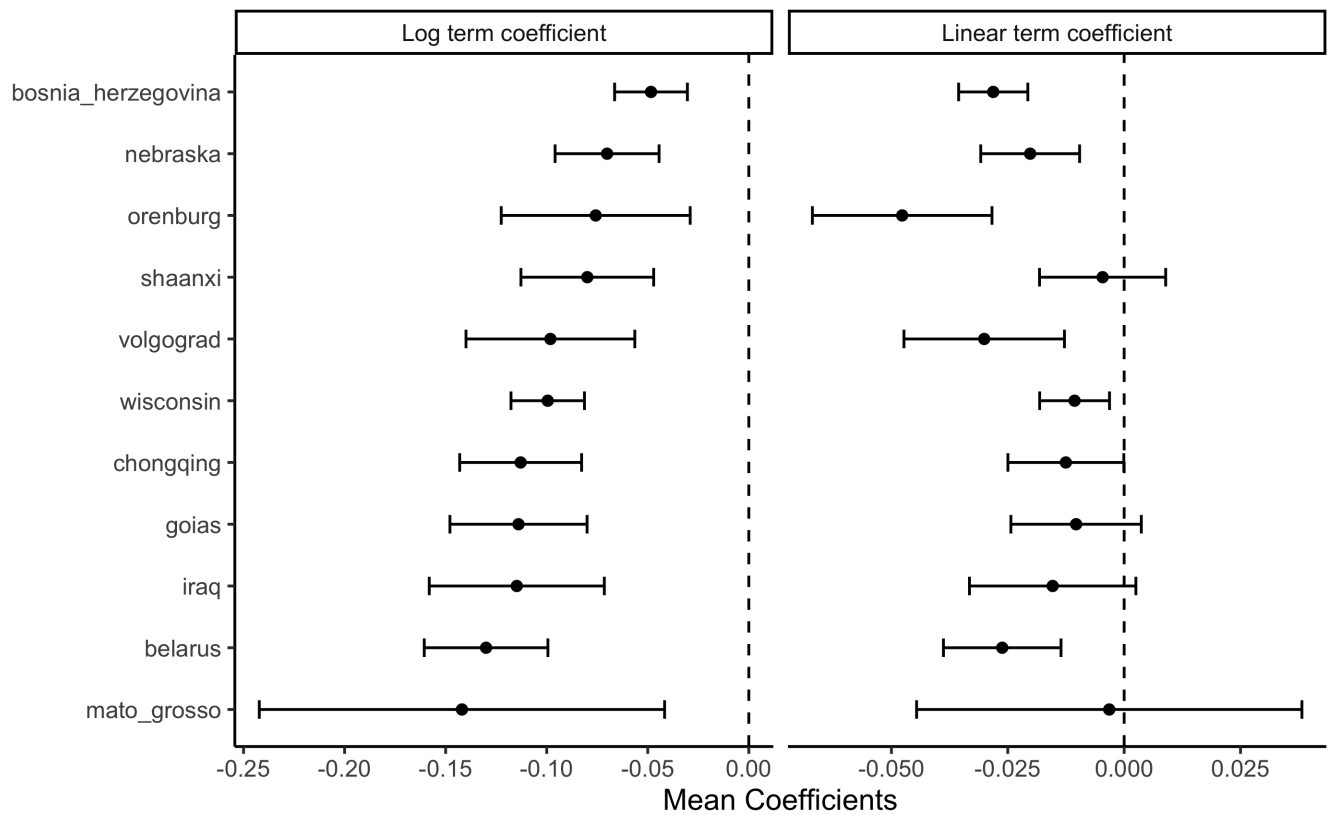


Fig. S16. Mean decay model coefficients across cohorts at each site. The left panel shows the mean coefficient on the $\log(\text{time})$ terms and the right shows the site mean coefficient on the linear time terms. These mean coefficients are used to plot the mean decay trajectories shown in Figure 3.

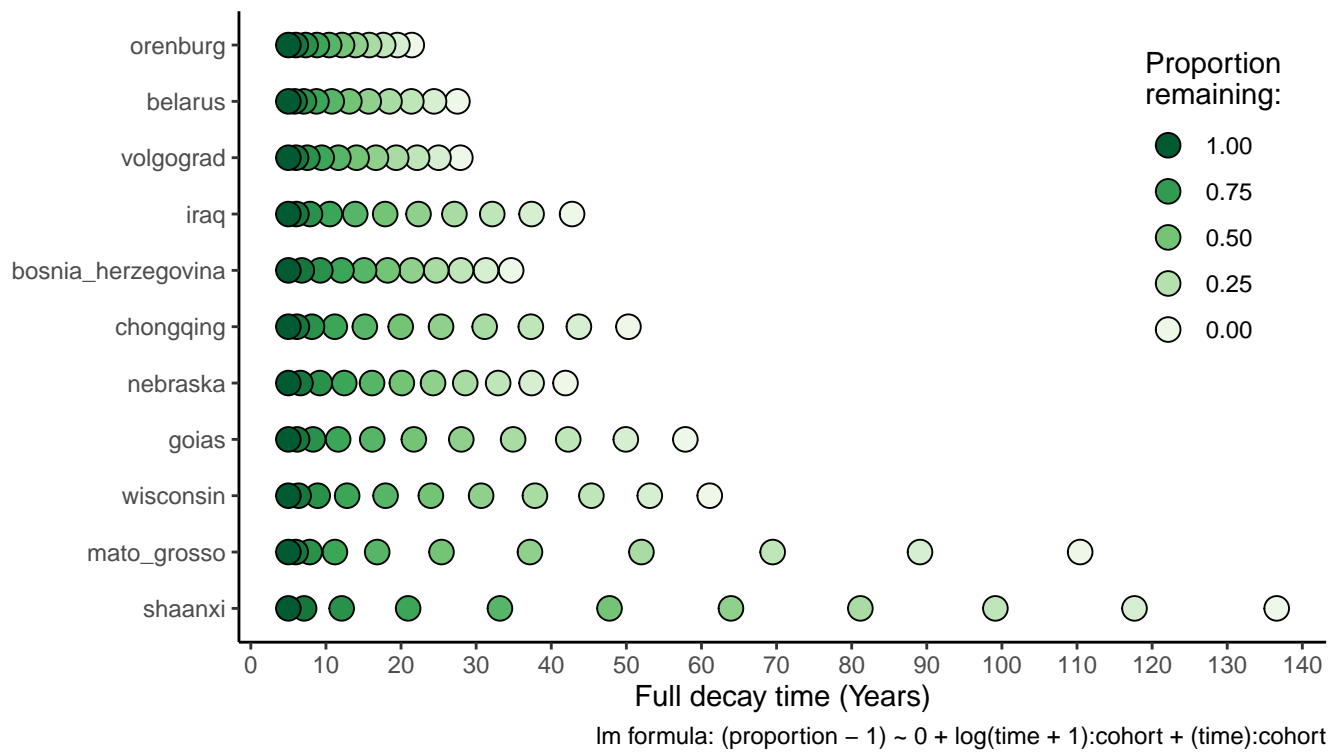


Fig. S17. An alternative representation of the mean decay rate for each site (also shown in Figure 3). The color of each point corresponds to the proportion remaining after a given amount of time.

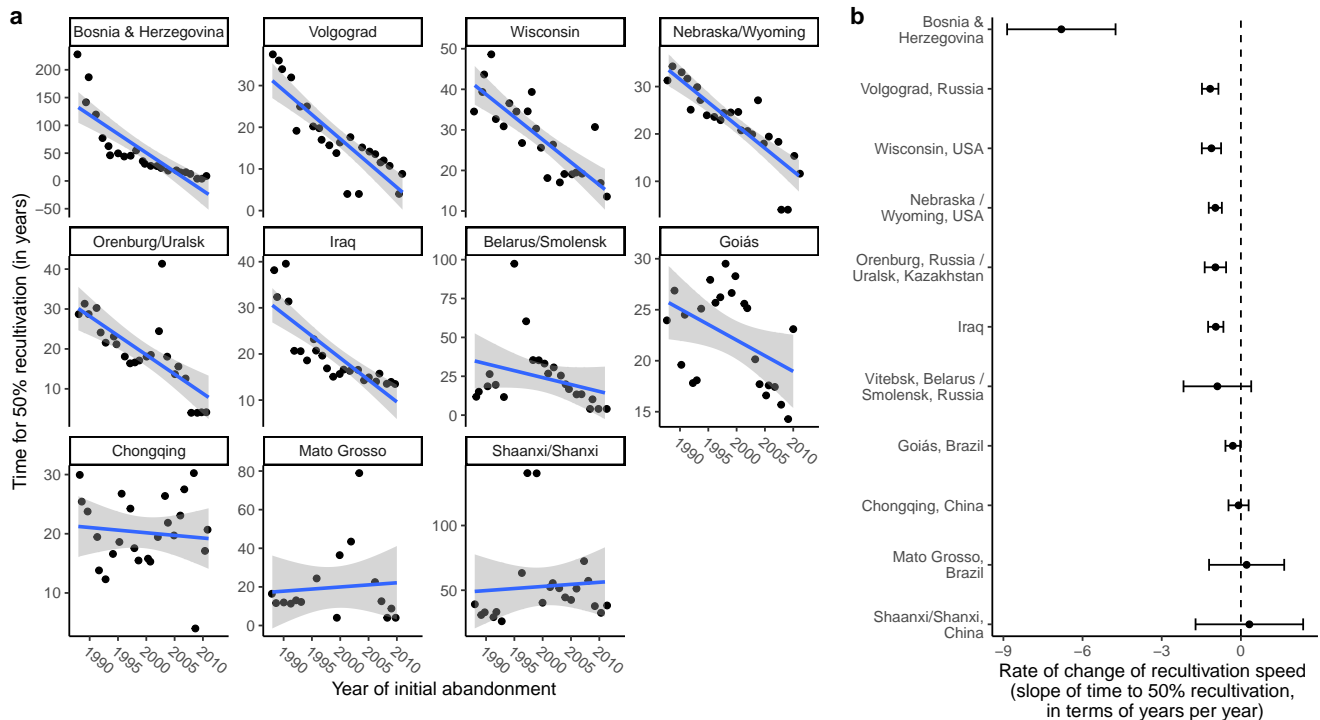


Fig. S18. The rate of change of decay rates (measured as the half-life, or the time required for 50% of each cohort to be recultivated) at each site over the course of the time series. Individual site trends are shown in panel a. Solid lines show simple linear regressions, the slopes of which are shown in panel b. Gray bands around the linear trends in panel a and the error bars on slope estimates in panel b both represent 95% confidence intervals. These models are described by Eq. Eq. (S3). Model diagnostic plots are shown in Figures S19 and S20.

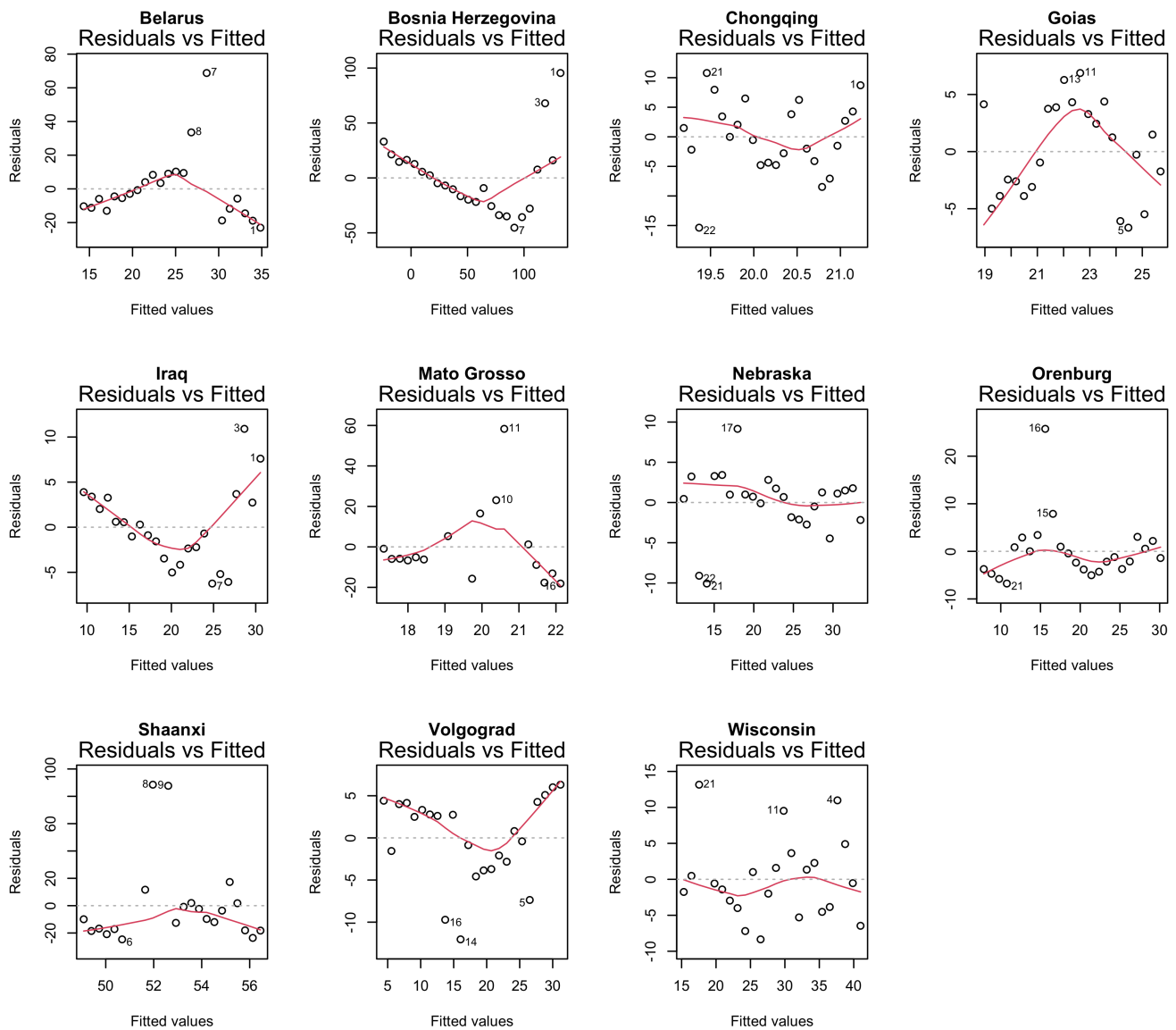


Fig. S19. Residuals vs. fitted diagnostic plots for each site, for a simple $1m$ call corresponding to Eq. Eq. (S3), in which the half-life (i.e., the time required for half (50%) of a given cohort of abandoned cropland to be recultivated) is modeled as a function of the year of initial abandonment at each site.

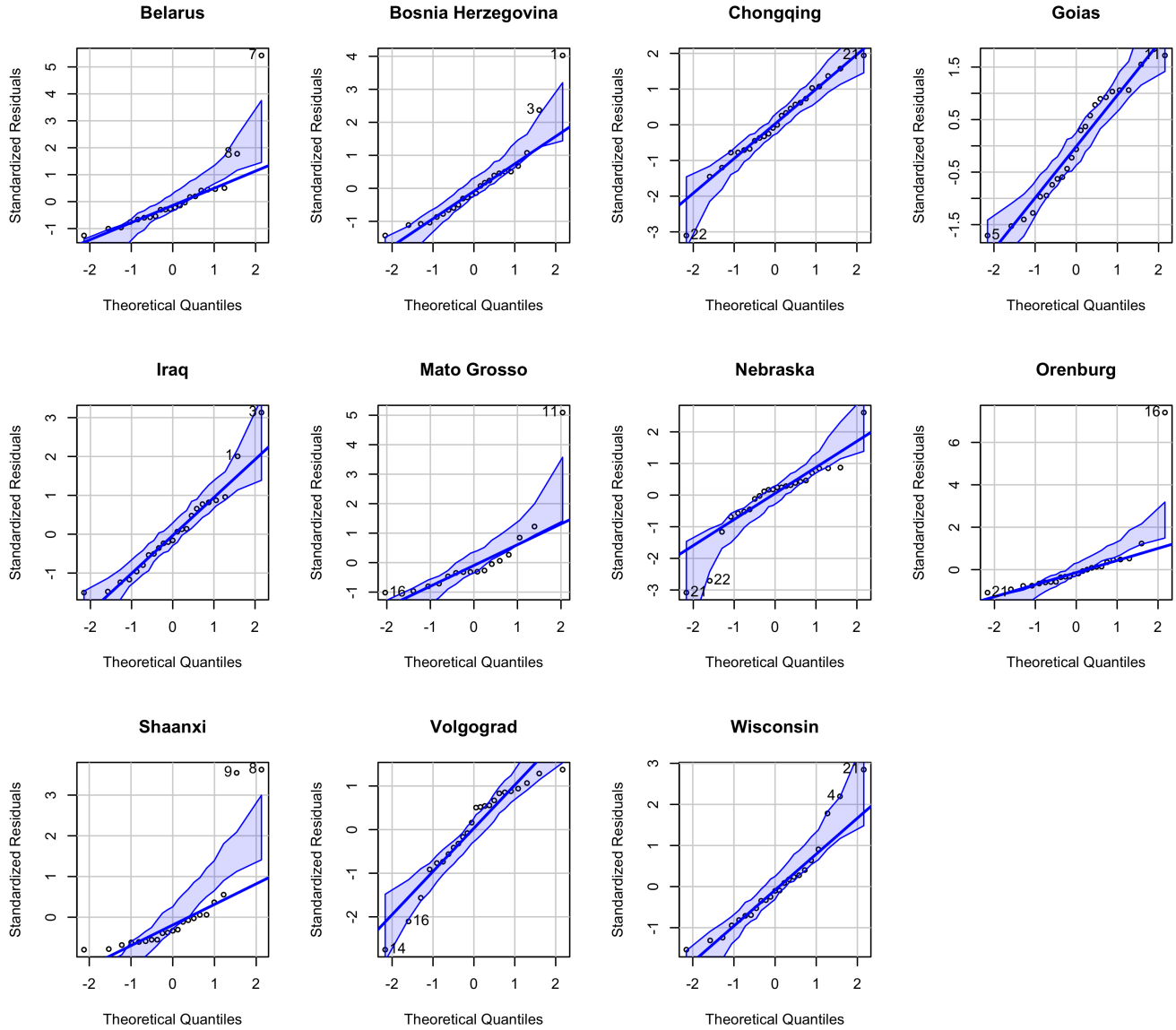


Fig. S20. QQ plots calculated using the `car` package ((14)), for a simple `1m` call corresponding to Eq. Eq. (S3), in which the half-life (i.e., the time required for half (50%) of a given cohort of abandoned cropland to be recultivated) is modeled as a function of the year of initial abandonment at each site.

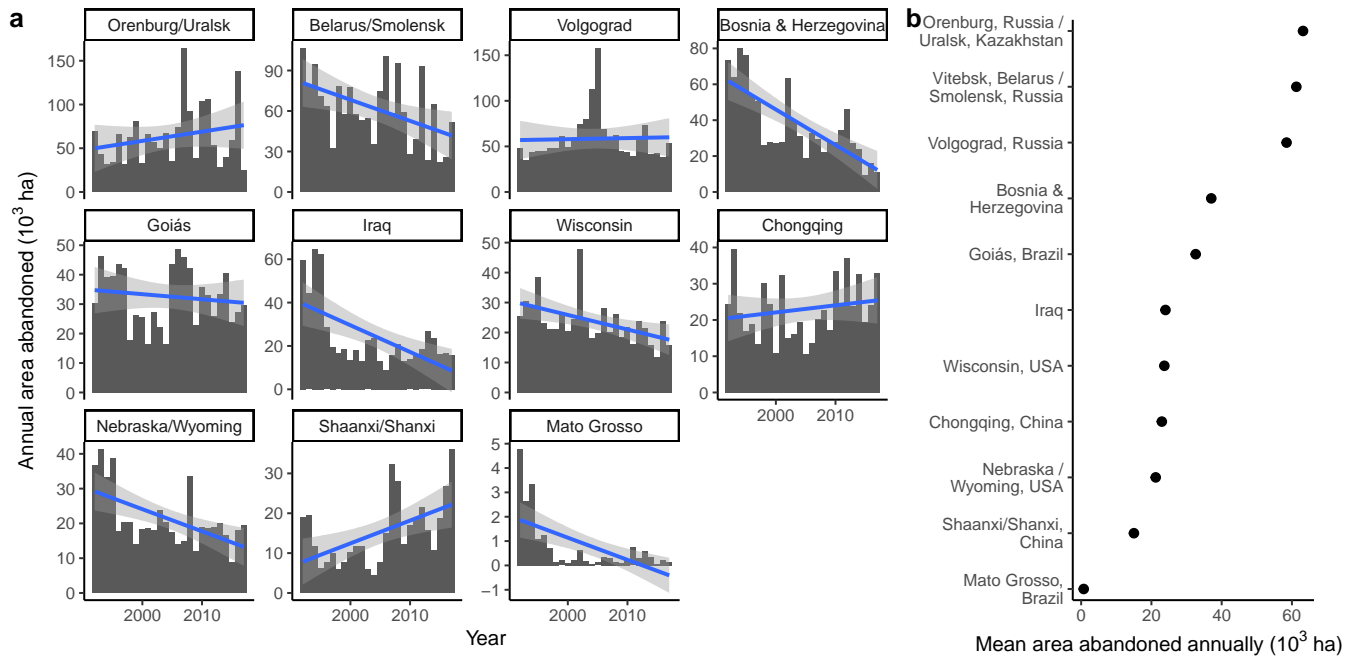


Fig. S21. Annual gain in newly abandoned cropland at our eleven sites. Panel a shows the trend in annual abandonment over time at each site (in 10^3 ha), and Panel b shows the mean annual abandonment (in 10^3 ha) at each site. The mean values in panel b feed into the extrapolations. Note that the annual gain in abandonment corresponds to the dark green bars in Figure S5.

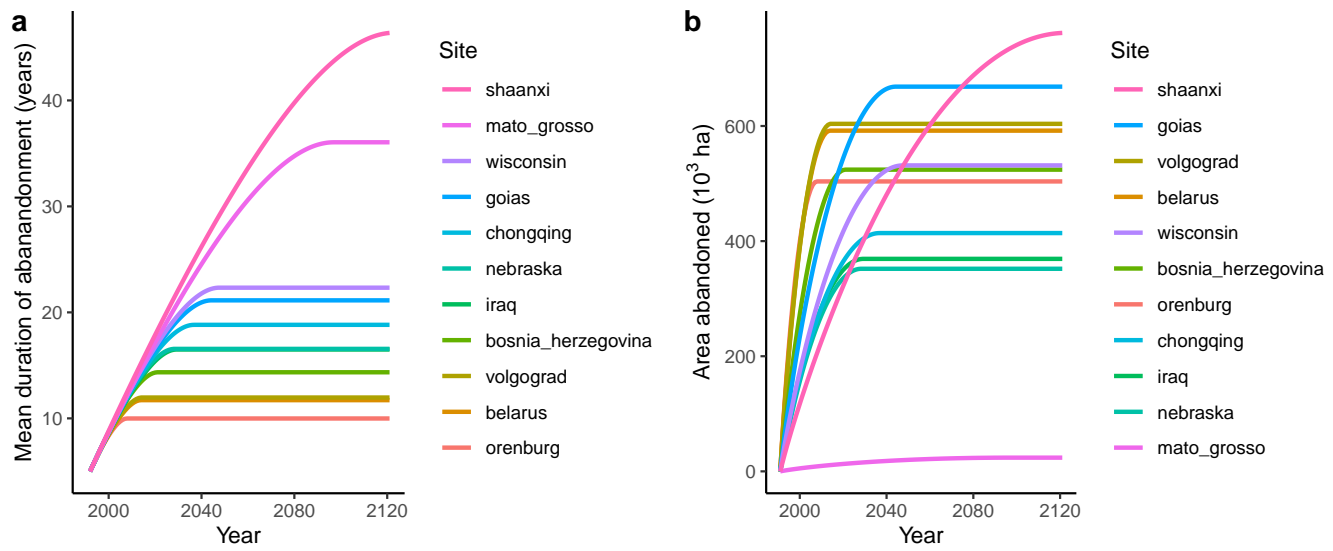


Fig. S22. The results of our simple extrapolation, including a) the mean age of abandonment, and b) the total area abandoned into the future. Colors corresponding to each site are consistent across the three panels. These extrapolations assume recultivation based on the mean decay trend for each site Figure 3 and annual new abandonment based on the mean annual gain in abandonment shown in Figure S5 (dark green bars).

Extrapolation 1

Assuming i) mean decay rates and ii) constant area abandoned each year.

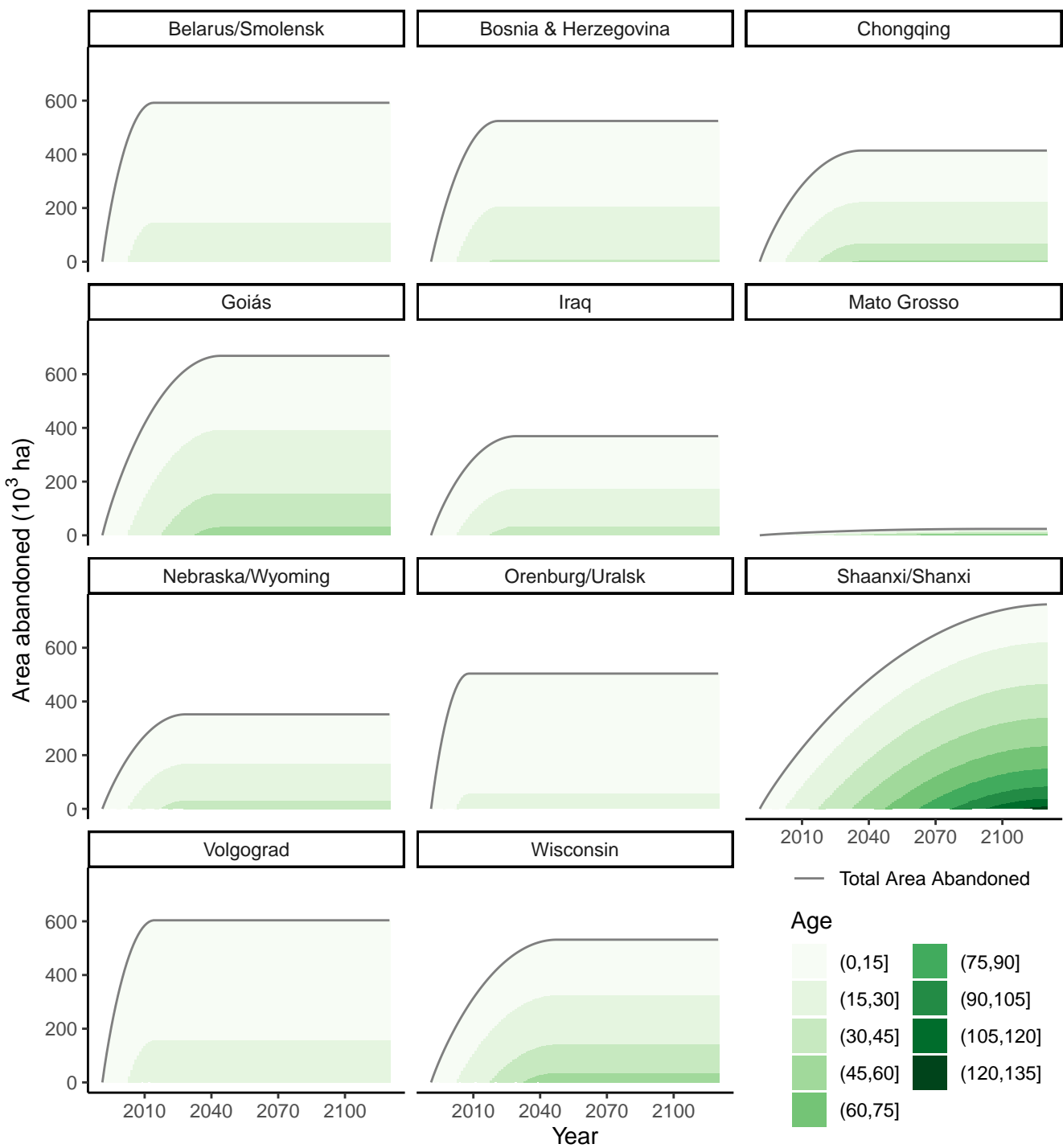


Fig. S23. Extrapolating area by age bin, assuming a 1) each site follows the mean recultivation ("decay") rate, and 2) a constant area abandoned each year (based on the mean annual area abandoned at each site).

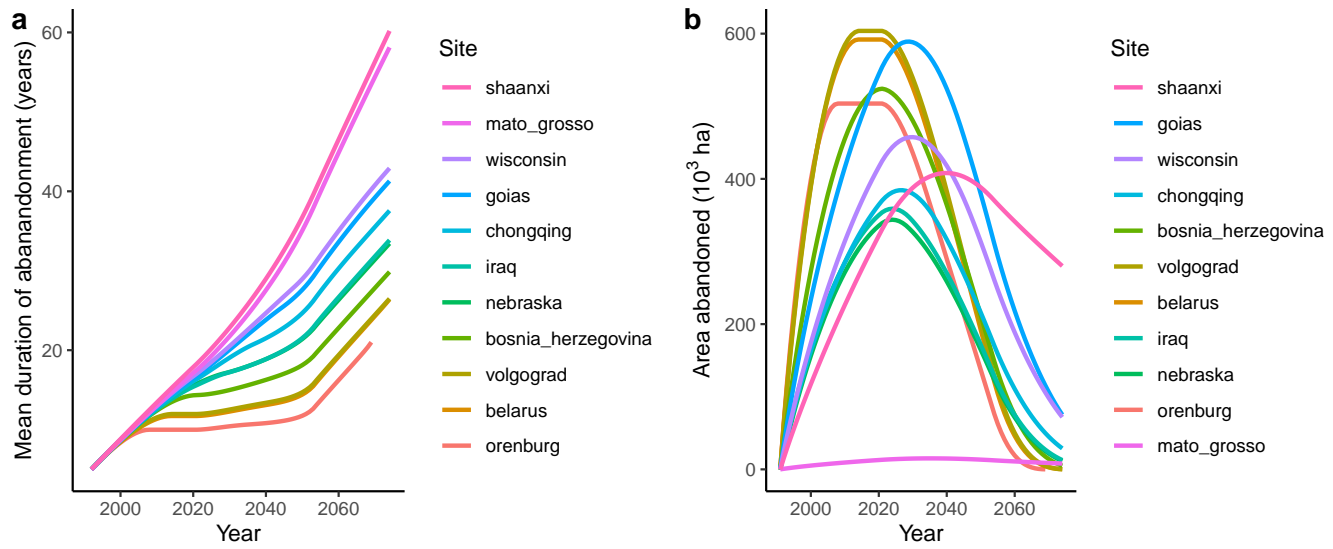


Fig. S24. The results of our second extrapolation, including a) the mean age of abandonment, and b) the total area abandoned into the future. Colors corresponding to each site are consistent across the three panels. These extrapolations assume recultivation based on the mean decay trend for each site (Figure 3) and annual new abandonment based on the mean annual gain in abandonment shown in Figure S5 (dark green bars).

Extrapolation 2

Assuming i) mean decay rates and ii) constant area abandoned each year until 2017, then linear decline in area abandoned each year until reaching 0 in 2050.

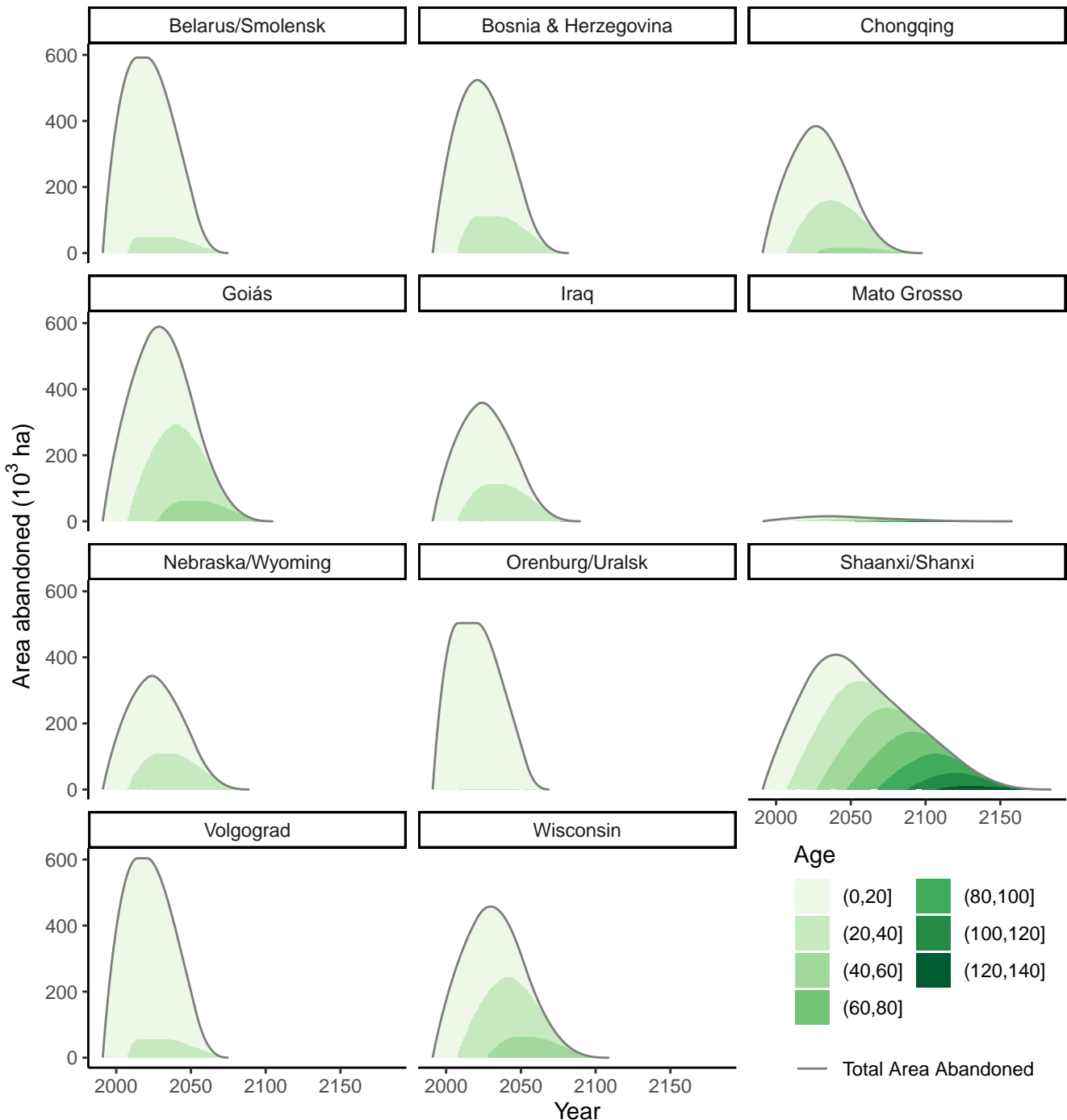


Fig. S25. Extrapolating area by age bin, assuming a 1) each site follows the mean recultivation ("decay") rate, and 2) a constant area abandoned each year until 2017 (based on the mean annual area abandoned at each site), followed by a linearly declining area abandoned each year until reaching 0 in 2050.

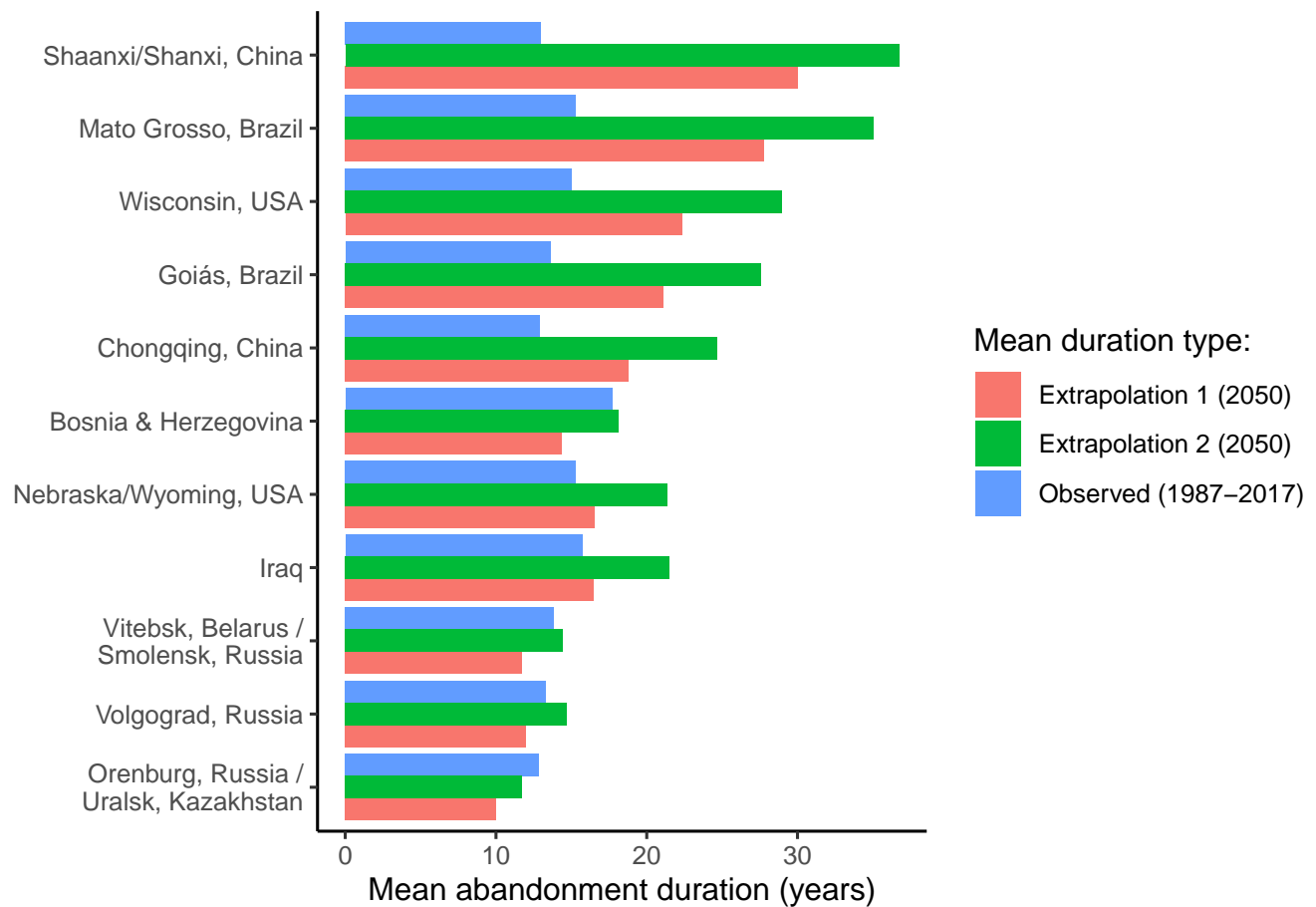


Fig. S26. Comparing the mean duration of abandonment at our 11 sites observed between 1987 and 2017 with the extrapolated mean duration as of 2050 for our two extrapolations.

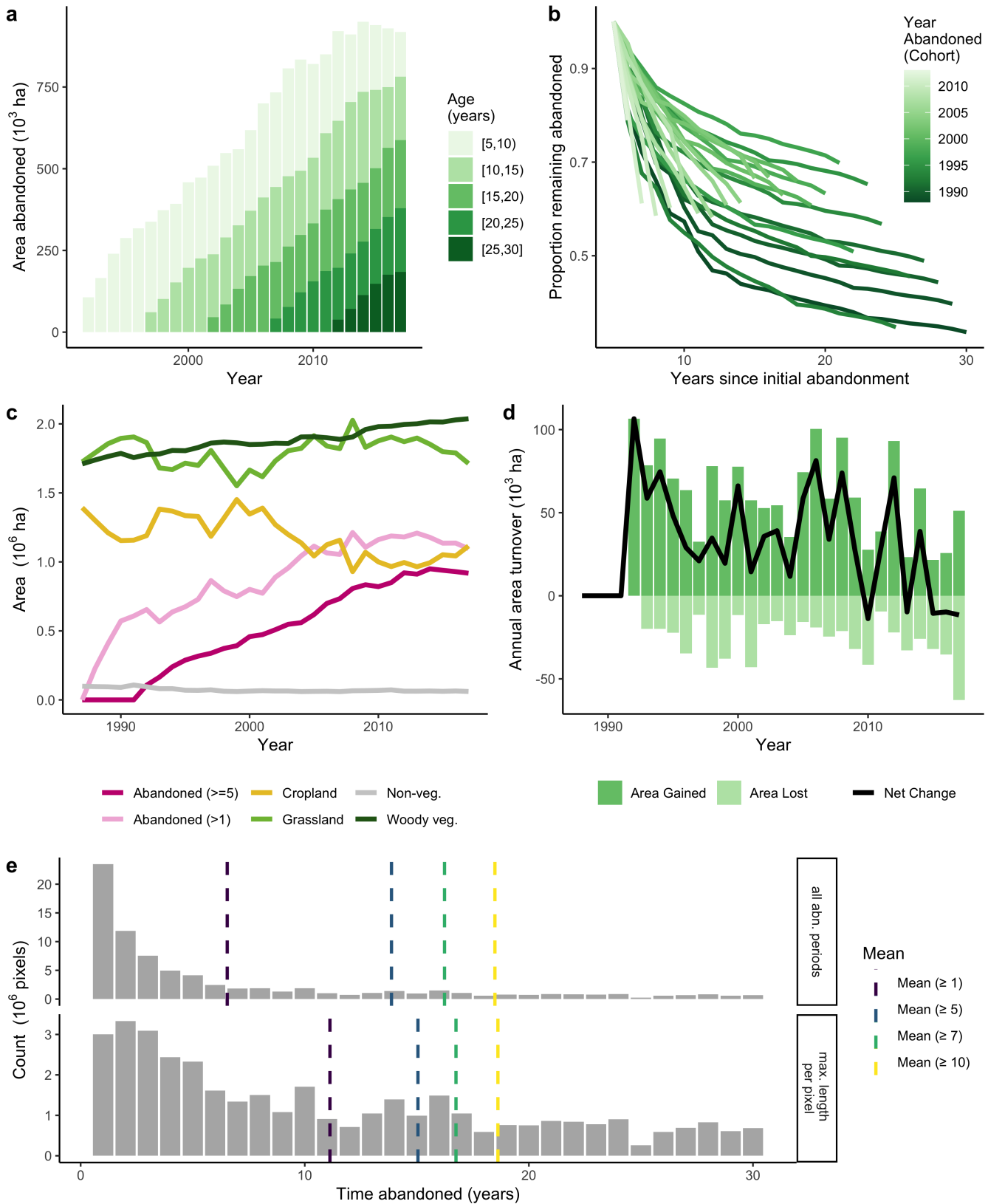


Fig. S27. Abandonment patterns for Vitebsk, Belarus / Smolensk, Russia, showing a) accumulation of abandoned land by age class, b) decay of abandoned land by year abandoned, c) the area in each land cover class through time (including both land that has been abandoned for five or more years, as well as any land abandoned for 1 or more years, therefore including short-term fallows), d) the annual turnover of abandoned land through time, and e) the distribution of abandonment duration for all periods of cropland abandonment (top) and the maximum duration of abandonment at each pixel (bottom).

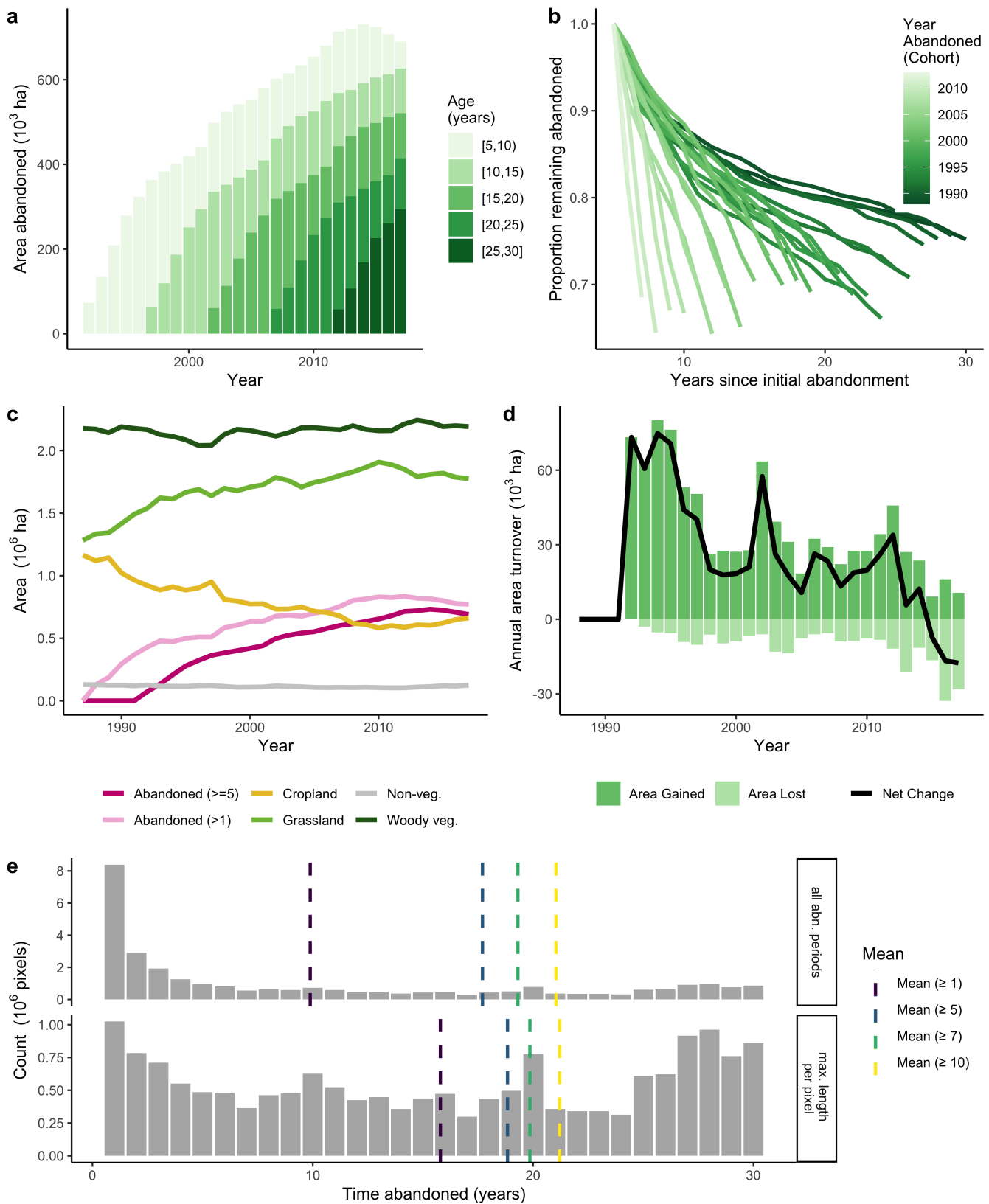


Fig. S28. Abandonment patterns for Bosnia & Herzegovina, following Figure S27.

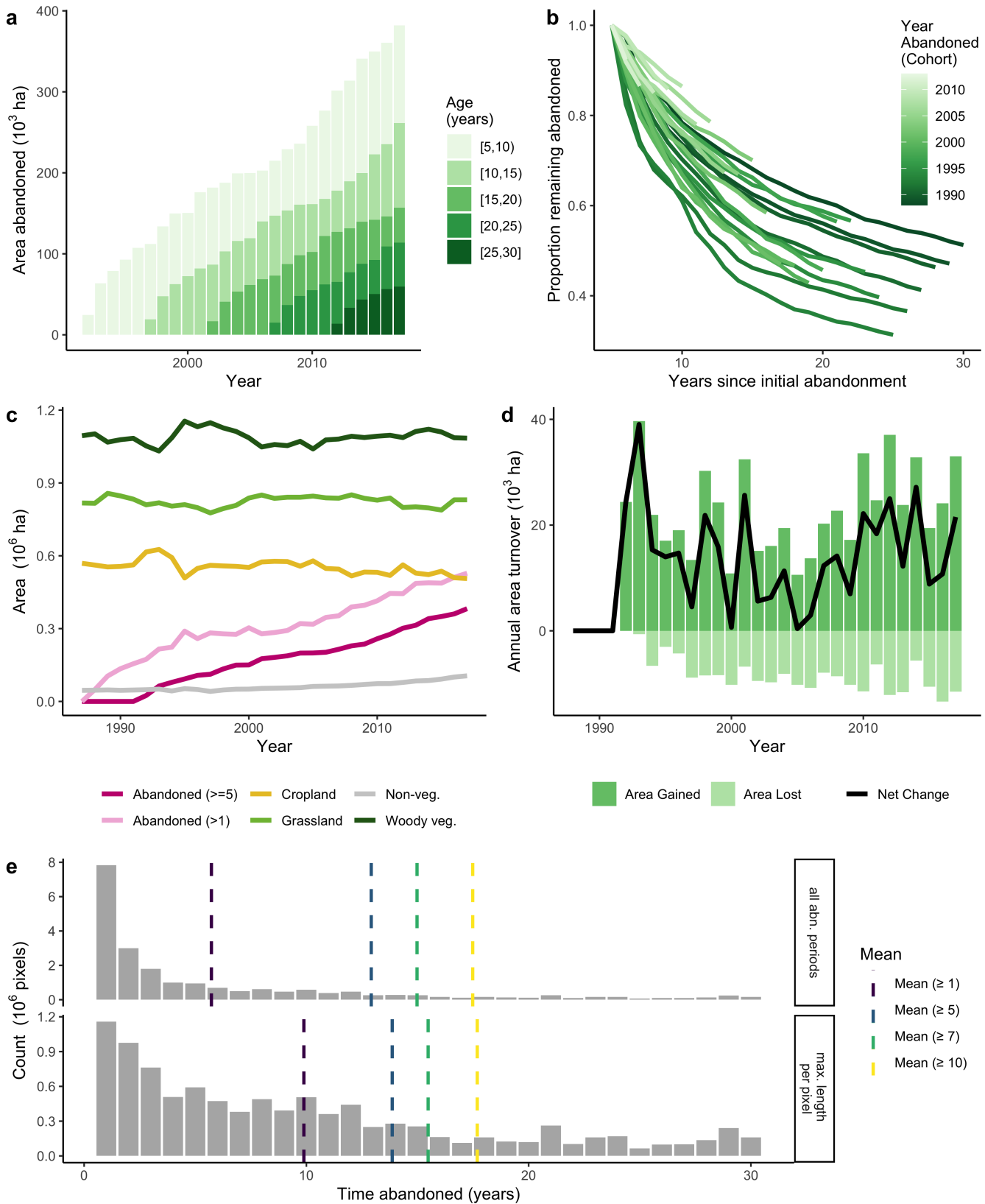


Fig. S29. Abandonment patterns for Chongqing, China, following Figure S27.

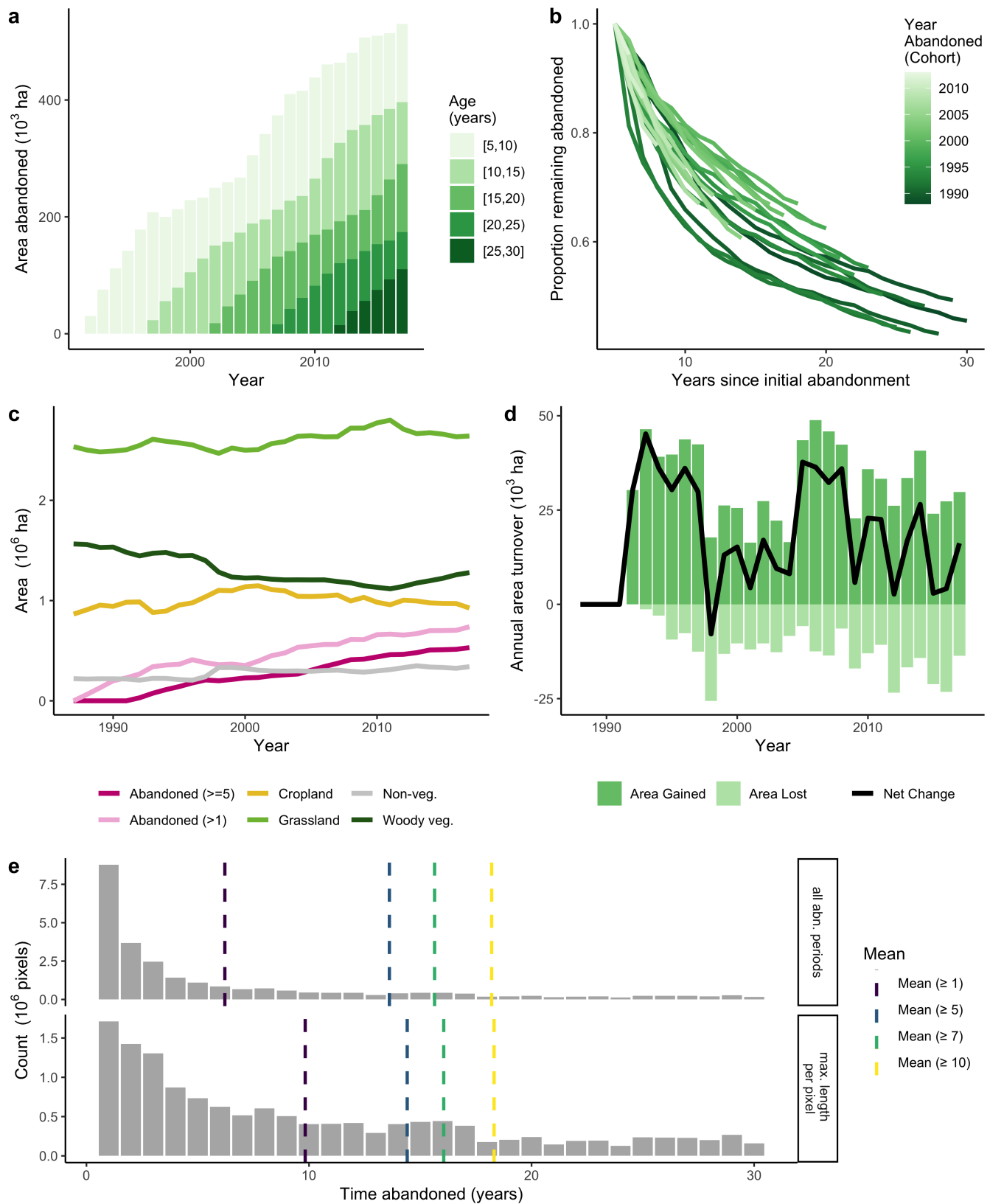


Fig. S30. Abandonment patterns for Goiás, Brazil, following Figure S27.

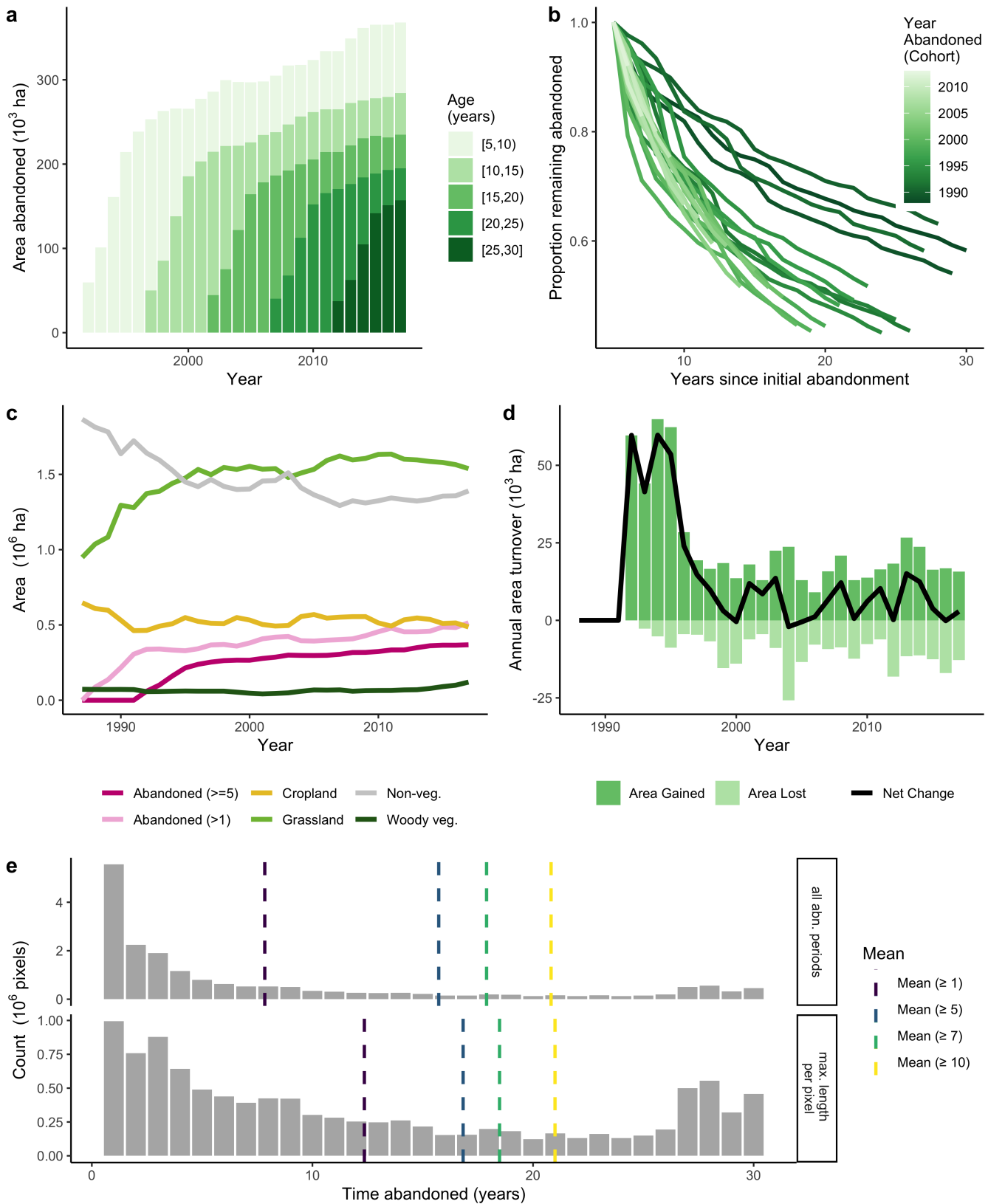


Fig. S31. Abandonment patterns for Iraq, following Figure S27.

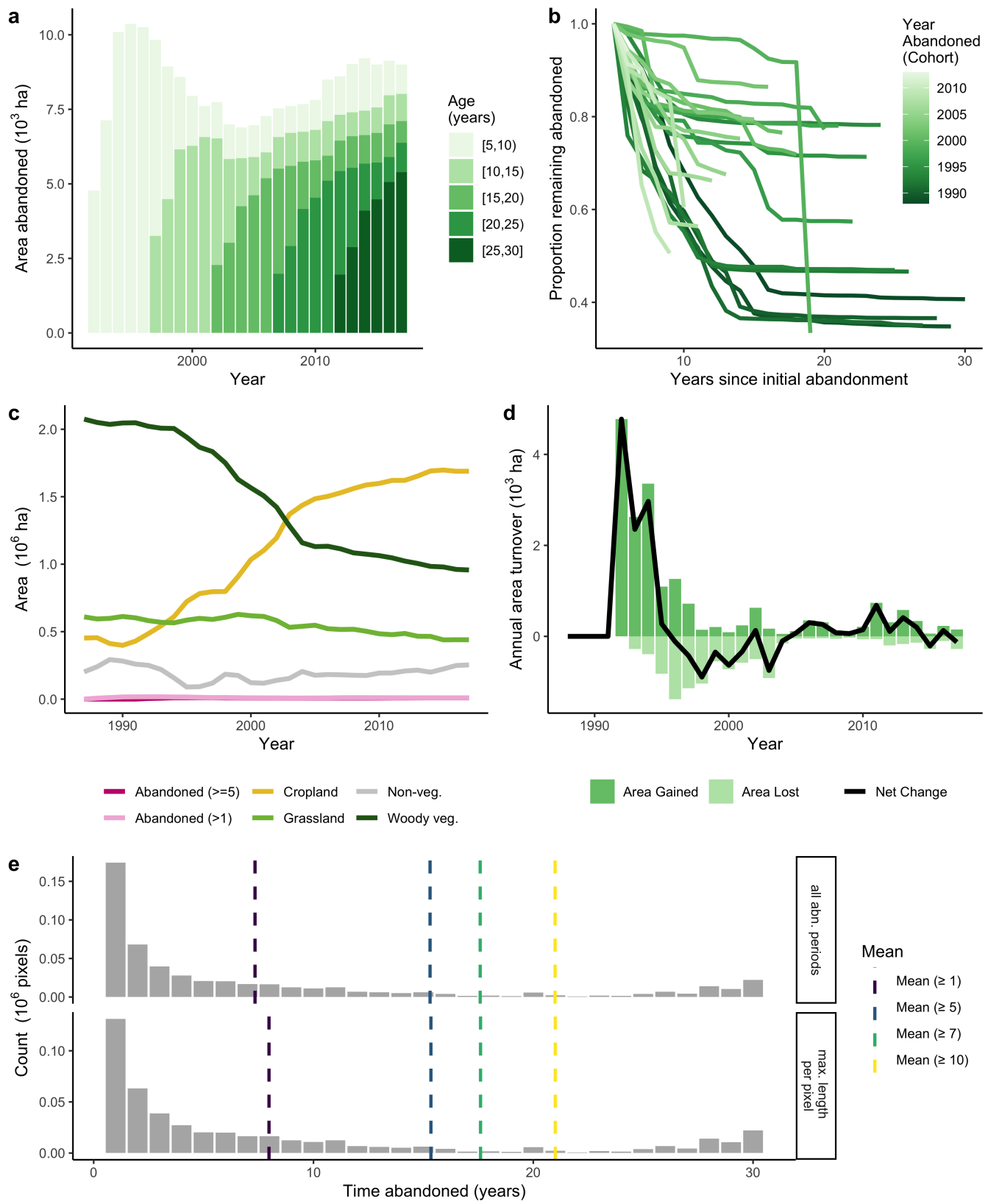


Fig. S32. Abandonment patterns for Mato Grosso, Brazil, following Figure S27.

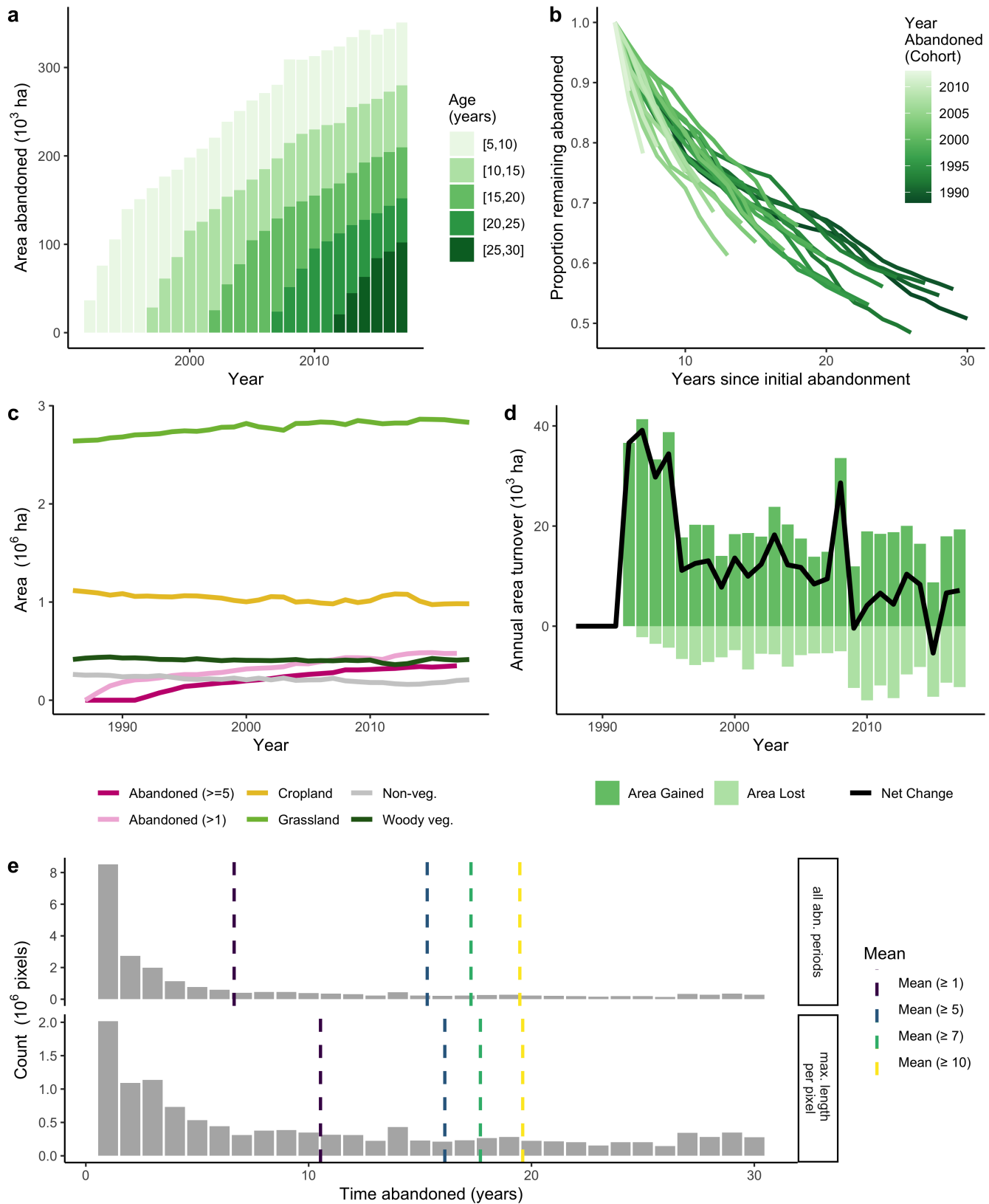


Fig. S33. Abandonment patterns for Nebraska/Wyoming, USA, following Figure S27.

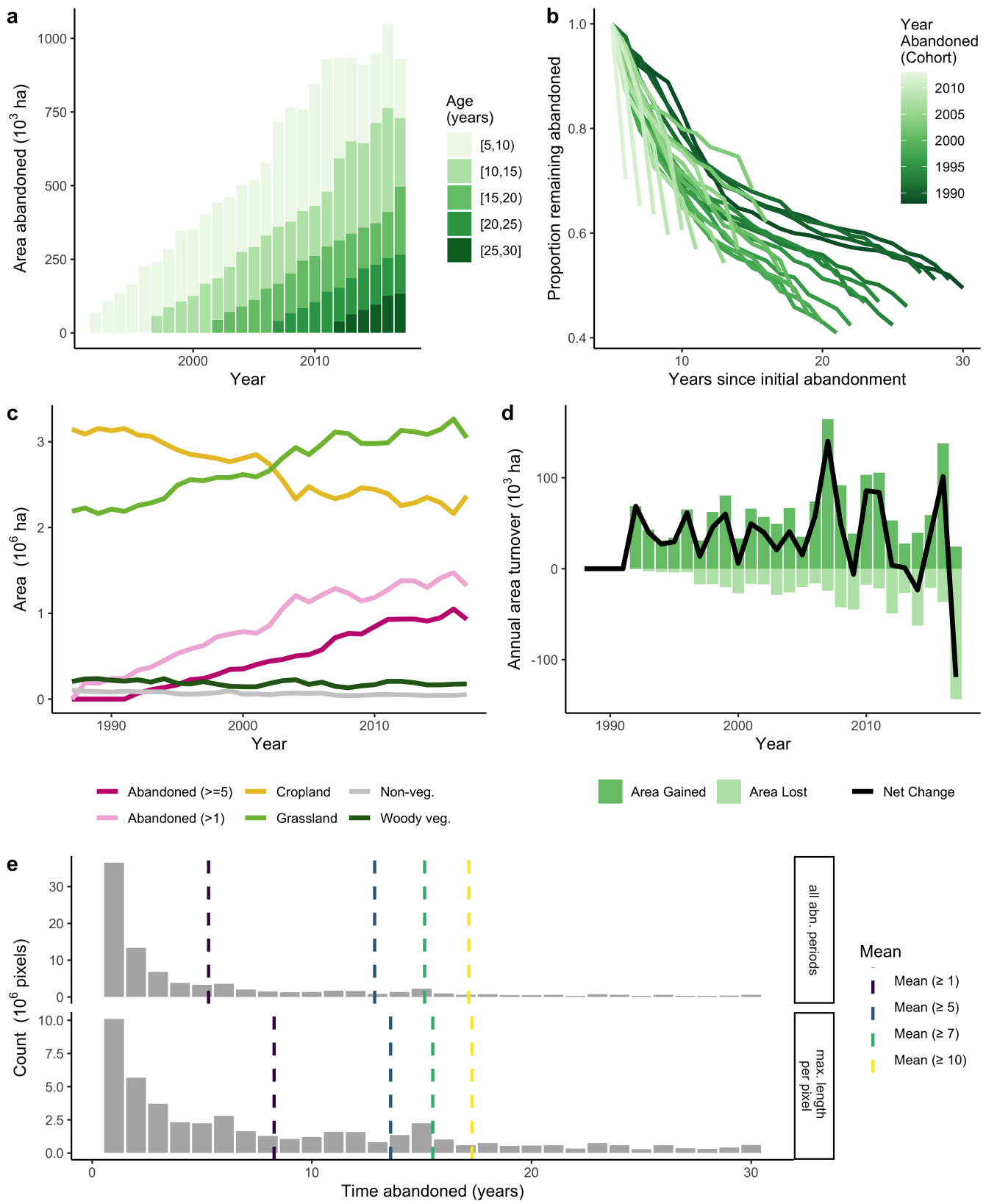


Fig. S34. Abandonment patterns for Orenburg, Russia / Uralsk, Kazakhstan, following Figure S27.

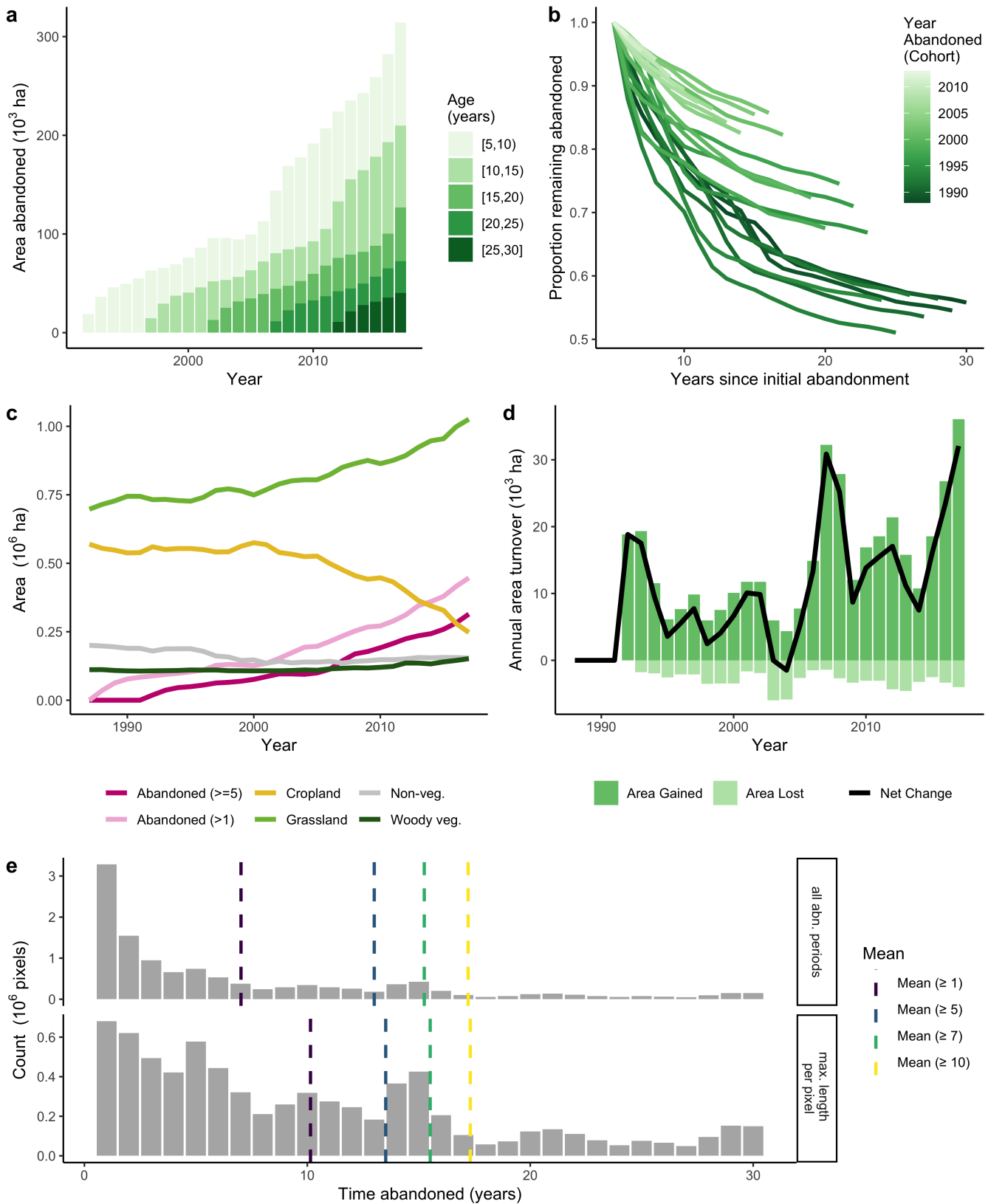


Fig. S35. Abandonment patterns for Shaanxi/Shanxi, China, following Figure S27.

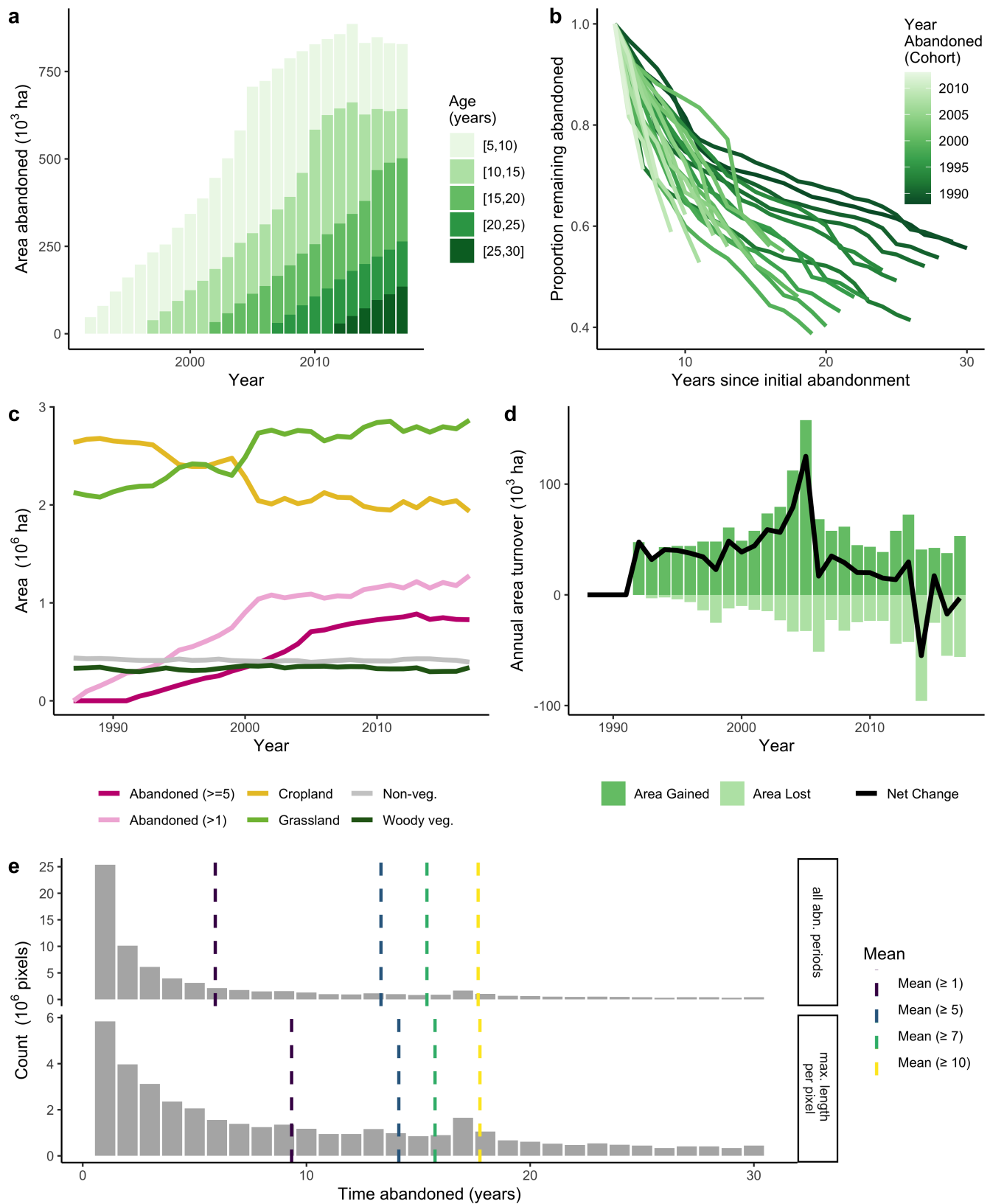


Fig. S36. Abandonment patterns for Volgograd, Russia, following Figure S27.

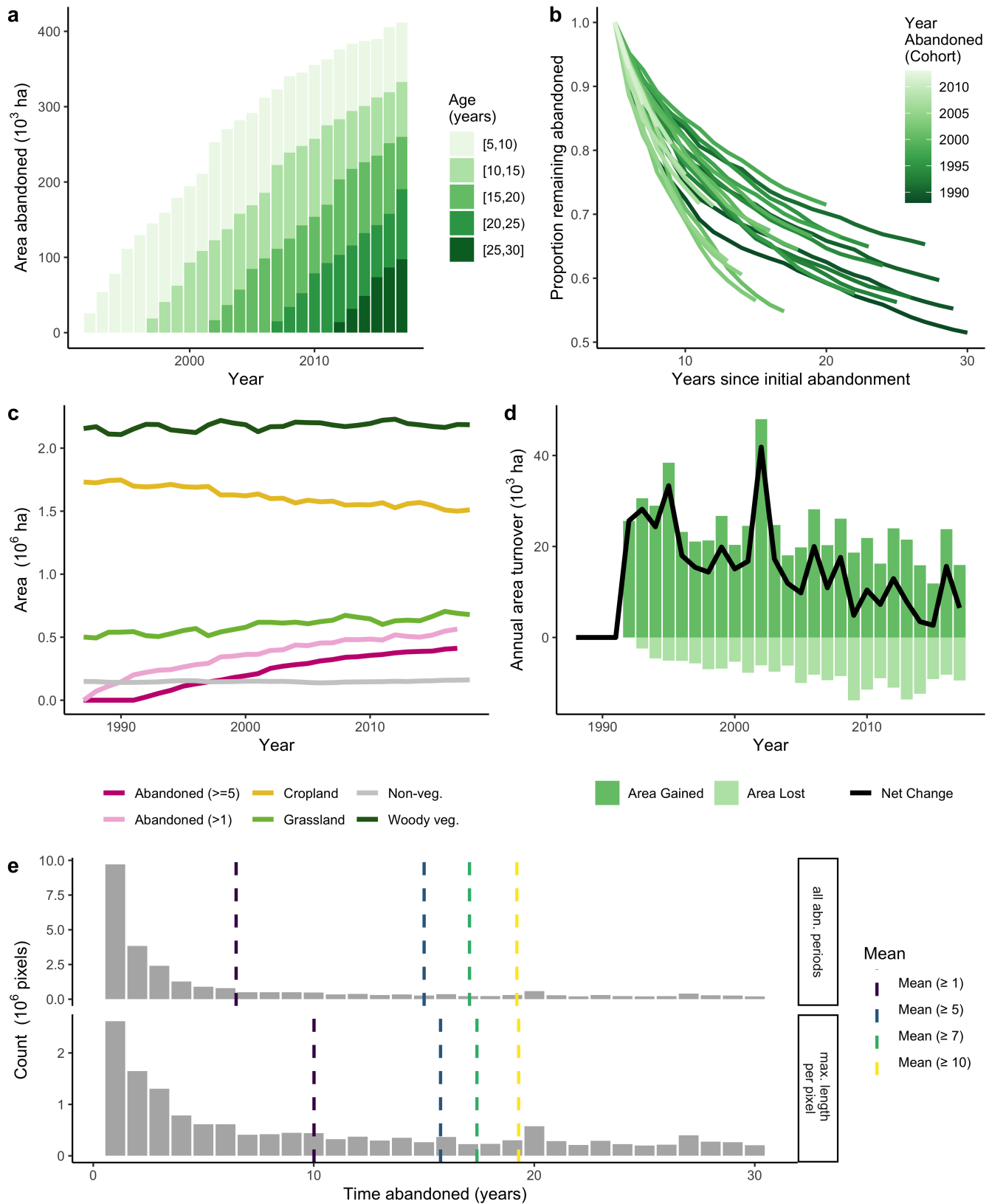


Fig. S37. Abandonment patterns for Wisconsin, USA, following Figure S27.

283 **References**

- 284 1. Prach K, Walker LR (2018) Differences between primary and secondary plant succession among biomes of the world.
285 *Journal of Ecology* (May 2018):510–516.
- 286 2. Munroe DK, Berkel DB van, Verburg PH, Olson JL (2013) Alternative trajectories of land abandonment: Causes,
287 consequences and research challenges. *Current Opinion in Environmental Sustainability* 5(5):471–476.
- 288 3. Food and Agriculture Organization of the United Nations (FAO) (2016) FAOSTAT Statistical Database: Methods &
289 Standards. Available at: <http://www.fao.org/ag/agn/nutrition/Indicatorsfiles/Agriculture.pdf>.
- 290 4. Næss JS, Cavalett O, Cherubini F (2021) The land–energy–water nexus of global bioenergy potentials from abandoned
291 cropland. *Nature Sustainability*. doi:[10.1038/s41893-020-00680-5](https://doi.org/10.1038/s41893-020-00680-5).
- 292 5. Legendre P, Legendre L (2012) *Numerical ecology*. (Boston: Elsevier). 3rd Ed.
- 293
- 294 6. Yin H, et al. (2020) Monitoring cropland abandonment with Landsat time series. *Remote Sensing of Environment*
295 246:111873.
- 296 7. RStudio Team (2020) RStudio: Integrated Development Environment for R. Available at: <http://www.rstudio.com/>.
- 297
- 298 8. Hijmans RJ (2021) *Raster: Geographic data analysis and modeling*. Available at: <https://rspatial.org/raster>.
- 299
- 300 9. Hijmans RJ (2021) *Terra: Spatial data analysis*. Available at: <https://rspatial.org/terra>.
- 301
- 302 10. Dowle M, Srinivasan A (2021) *Data.table: Extension of ‘data.frame’*. Available at: <https://CRAN.R-project.org/package=data.table>.
- 303
- 304 11. Wickham H (2021) *Tidyverse: Easily install and load the tidyverse*. Available at: <https://CRAN.R-project.org/package=tidyverse>.
- 305
- 306 12. Olson DM, et al. (2001) Terrestrial Ecoregions of the World: A New Map of Life on Earth. *BioScience* 51(11):933–938.
- 307
- 308 13. Olson DM, Dinerstein E (2002) The Global 200: Priority ecoregions for global conservation. *Annals of the Missouri*
309 *Botanical Garden* 89(2):199–224.
- 310 14. Fox J, Weisberg S, Price B (2021) *Car: Companion to applied regression*. Available at: <https://CRAN.R-project.org/package=car>.
- 311